Thermodynamics in the vicinity of a relativistic quantum critical point in 2 + 1 dimensions

A. Rançon,[1,2] O. Kodio,[2] N. Dupuis,[2] and P. Lecheminant[3]

[1]*James Franck Institute and Department of Physics, University of Chicago, Chicago, Illinois 60637, USA*

[2]*Laboratoire de Physique Théorique de la Matière Condensée, CNRS UMR 7600, Université Pierre et Marie Curie, 4 Place Jussieu, 75252 Paris Cedex 05, France*

[3]*Laboratoire de Physique Théorique et Modélisation, CNRS UMR 8089, Université de Cergy-Pontoise, Site de Saint-Martin, 2 avenue Adolphe Chauvin, 95302 Cergy-Pontoise Cedex, France*

(Received 26 March 2013; published 15 July 2013)

We study the thermodynamics of the relativistic quantum O(N) model in two space dimensions. In the vicinity of the zero-temperature quantum critical point (QCP), the pressure can be written in the scaling form $P(T) = P(0) + N(T^3/c^2)\mathcal{F}_N(\Delta/T)$, where c is the velocity of the excitations at the QCP and $|\Delta|$ a characteristic zero-temperature energy scale. Using both a large-N approach to leading order and the nonperturbative renormalization group, we compute the universal scaling function $\mathcal{F}_N$. For small values of N ($N \lesssim 10$) we find that $\mathcal{F}_N(x)$ is nonmonotonic in the quantum critical regime ($|x| \lesssim 1$) with a maximum near $x = 0$. The large-N approach—if properly interpreted—is a good approximation both in the renormalized classical ($x \lesssim -1$) and quantum disordered ($x \gtrsim 1$) regimes, but fails to describe the nonmonotonic behavior of $\mathcal{F}_N$ in the quantum critical regime. We discuss the renormalization-group flows in the various regimes near the QCP and make the connection with the quantum nonlinear sigma model in the renormalized classical regime. We compute the Berezinskii-Kosterlitz-Thouless transition temperature in the quantum O(2) model and find that in the vicinity of the QCP the universal ratio $T_{\rm BKT}/\rho_s(0)$ is very close to $\pi/2$, implying that the stiffness $\rho_s(T_{\rm BKT}^-)$ at the transition is only slightly reduced with respect to the zero-temperature stiffness $\rho_s(0)$. Finally, we briefly discuss the experimental determination of the universal function $\mathcal{F}_2$ from the pressure of a Bose gas in an optical lattice near the superfluid–Mott-insulator transition.

DOI: 10.1103/PhysRevE.88.012113 PACS number(s): 05.30.Rt, 67.85.−d

I. INTRODUCTION

Many zero-temperature critical points observed in quantum many-body systems are described by a relativistic effective field theory [1,2]. Bosonic cold atomic gases constitute a very clean experimental realization of such quantum critical points (QCPs): A Bose gas in an optical lattice undergoes a quantum phase transition between a Mott insulator and a superfluid state [3–6]. When the transition occurs at fixed density, it is described by a relativistic quantum O(2) model [7,8].

Recent works have focused on the excitation spectrum of the relativistic quantum O(N) model in the vicinity of the QCP and in particular on the spectral function of the amplitude ("Higgs") mode in the broken-symmetry phase [2,9–12]. Signatures of the amplitude mode have recently been observed in a two-dimensional superfluid near the superfluid–Mott-insulator transition [13].

In this paper, we study the thermodynamics of the relativistic quantum O(N) model in two space dimensions. We extend previous results [1,14] obtained to leading order in the large-N limit by computing the full scaling function $\mathcal{F}_\infty(x)$ determining the temperature dependence of the pressure near the QCP. Using a nonperturbative renormalization-group (NPRG) approach [15–17], we then calculate $\mathcal{F}_N(x)$ for finite values of N, including $N = 2$ and $N = 3$.

We start from the action

$$S[\boldsymbol{\varphi}] = \int dx \left\{ \frac{1}{2}(\nabla\boldsymbol{\varphi})^2 + \frac{1}{2c_0^2}(\partial_\tau\boldsymbol{\varphi})^2 + \frac{r_0}{2}\boldsymbol{\varphi}^2 + \frac{u_0}{4!N}(\boldsymbol{\varphi}^2)^2 \right\}, \tag{1}$$

where we use the shorthand notation

$$x = (\mathbf{r},\tau), \quad \int dx = \int_0^\beta d\tau \int d^2r. \tag{2}$$

$\boldsymbol{\varphi}(x)$ is an N-component real field and $\tau \in [0,\beta]$ an imaginary time ($\beta = 1/T$ and we set $\hbar = k_B = 1$). r_0 and u_0 are temperature-independent coupling constants and c_0 is the (bare) velocity of the $\boldsymbol{\varphi}$ field. The factor $1/N$ in Eq. (1) is introduced to obtain a meaningful limit $N \to \infty$ (with u_0 fixed). The model is regularized by an ultraviolet cutoff Λ. In order to maintain the Lorentz invariance of the action (1) at zero temperature, it is natural to implement a cutoff on both momenta and frequencies but we will also sometimes use a cutoff acting only on momenta.

In two space dimensions, the phase diagram of the relativistic quantum O(N) model is well known (Fig. 1) [1]. At zero temperature, there is a quantum phase transition between a disordered phase ($r_0 > r_{0c}$) and an ordered phase ($r_0 < r_{0c}$) where the O(N) symmetry of the action (1) is spontaneously broken (u_0 and c_0 are considered as fixed parameters). The QCP at $r_0 = r_{0c}$ is in the universality class of the three-dimensional classical O(N) model with a dynamical critical exponent $z = 1$ (this value follows from Lorentz invariance at zero temperature); the phase transition is governed by the three-dimensional Wilson-Fisher fixed point. At finite temperatures, the system is always disordered for $N \geqslant 2$, in agreement with the Mermin-Wagner theorem, but it is possible to distinguish three regimes in the vicinity of the QCP: a renormalized classical regime, a quantum critical regime, and a quantum disordered regime [1,18]. For $N = 2$ and $r_0 < r_{0c}$, there is a finite-temperature Berezinskii-Kosterlitz-Thouless

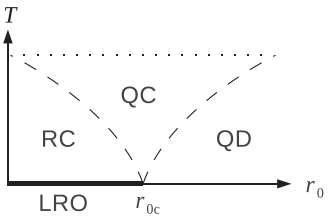

FIG. 1. Phase diagram of the relativistic O(N) model in two space dimensions for $N \geqslant 3$ [Eq. (1)]. The thick line shows the zero-temperature ordered phase with long-range order (LRO), while the dashed lines are crossover lines between the renormalized classical (RC), quantum critical (QC), and quantum disordered (QD) regimes. The dotted line shows the limit of the high-T region where the physics is not controlled by the QCP anymore. (For $N = 2$, there is a finite-temperature BKT transition line for $r_0 \leqslant r_{0c}$, which terminates at $T = 0$ for $r_0 = r_{0c}$.)

(BKT) phase transition [19–21] and the system exhibits algebraic order at low temperatures. The BKT transition temperature line $T_{\rm BKT}$ terminates at the QCP $r_0 = r_{0c}$.

Below the upper critical dimension $d_c^+ = 3$ ($d_c^+ + z = 4$) of the quantum phase transition, we expect the hyperscaling hypothesis to hold. In two dimensions, this allows us to write the pressure in the critical regime as [22]

$$P(T) = P(0) + N\frac{T^3}{c^2}\mathcal{F}_N\left(\frac{\Delta}{T}\right), \tag{3}$$

where $\mathcal{F}_N$ is a universal scaling function, c the velocity of the critical fluctuations at the QCP [23], and $|\Delta| \equiv |\Delta(r_0)|$ a characteristic energy scale at zero temperature. When $r_0 > r_{0c}$, the system is disordered and we choose Δ to be equal to the excitation gap $m_0 \propto (r_0 - r_{0c})^{z\nu}$ of the $\boldsymbol{\varphi}$ field (ν denotes the correlation-length exponent at the QCP)—not to be confused with the amplitude ("Higgs") mode gap. When $r_0 < r_{0c}$ it is convenient to take Δ negative such that $-\Delta$ is the excitation gap in the disordered phase at the point located symmetrically with respect to the QCP; i.e., $|\Delta(r_0)| = m_0(2r_{0c} - r_0)$ [2]. $-\Delta$ is then proportional to the stiffness ρ_s, the ratio $|\Delta|/\rho_s$ being universal. With these definitions, Δ varies from negative to positive values as we go across the QCP coming from the ordered phase. The two crossover lines shown in Fig. 1 are roughly defined by $|\Delta| \sim T$. We stress that the scaling function $\mathcal{F}_N$ is independent of all microscopic parameters of the model such as r_0, u_0, or c_0. The latter enter the temperature variation of the pressure [Eq. (3)] only indirectly *via* the values of the renormalized velocity c and the energy scale Δ.

In the critical regime near the QCP, all thermodynamic quantities can be written in a scaling form. In addition to $\mathcal{F}_N$, we will compute the universal scaling function F_N which determines the excitation gap

$$m(T) = T F_N\left(\frac{\Delta}{T}\right) \tag{4}$$

at finite temperatures. As we shall see, the knowledge of F_N is necessary to obtain $\mathcal{F}_N$ in the large-N limit.

The outline of the paper is as follows. In Sec. II, we compute the universal scaling functions F_N and $\mathcal{F}_N$ to leading order in a $1/N$ expansion. We then use a NPRG approach to calculate F_N and $\mathcal{F}_N$ for any value $N \geqslant 2$ (Sec. III). The main results are presented in Sec. III B. Section III C is devoted to a detailed analysis of the RG flows in the renormalized classical, quantum disordered, and quantum critical regimes for $N \geqslant 3$. In the renormalized classical regime, where the physics is dominated by the $N - 1$ Goldstone modes of the zero-temperature broken-symmetry phase, we show that the NPRG flow equations yield the one-loop RG equations of the quantum O(N) nonlinear σ model (NLσM) [18]. The BKT transition temperature in the quantum O(2) model is discussed in Sec. III E. The implication of our results for cold atomic gases are briefly discussed in the Conclusion.

II. LARGE-N LIMIT

In this section, we use a cutoff Λ acting only on momenta; i.e., $|\mathbf{q}| \leqslant \Lambda$. We do not distinguish between the bare velocity c_0 and the renormalized one c since they coincide in the large-N limit.

Following the standard method in the large-N limit (see, e.g., Refs. [24,25]), we express the partition function as

$$Z = \int \mathcal{D}[\boldsymbol{\varphi},\rho,\lambda] \exp\left\{-\int dx\left[\frac{1}{2}(\boldsymbol{\nabla}\boldsymbol{\varphi})^2 + \frac{1}{2c^2}(\partial_\tau\boldsymbol{\varphi})^2 + \frac{r_0}{2}\rho + \frac{u_0}{4!N}\rho^2 + i\frac{\lambda}{2}(\boldsymbol{\varphi}^2 - \rho)\right]\right\}. \tag{5}$$

It can be easily verified that by integrating out λ and then ρ, one recovers the original action $S[\boldsymbol{\varphi}]$. If, instead, we first integrate out ρ, we obtain

$$Z = \int \mathcal{D}[\boldsymbol{\varphi},\lambda] \exp\left\{-\int dx\left[\frac{1}{2}(\boldsymbol{\nabla}\boldsymbol{\varphi})^2 + \frac{1}{2c^2}(\partial_\tau\boldsymbol{\varphi})^2 + i\frac{\lambda}{2}\boldsymbol{\varphi}^2\right] + \frac{3N}{2u_0}\int dx\,(i\lambda - r_0)^2\right\}. \tag{6}$$

We then split the $\boldsymbol{\varphi}$ field into a field σ and a $(N-1)$-component field $\boldsymbol{\pi}$. The integration over the $\boldsymbol{\pi}$ field gives

$$\int \mathcal{D}[\boldsymbol{\pi}] \exp\left\{-\int dx\left[\frac{1}{2}(\boldsymbol{\nabla}\boldsymbol{\pi})^2 + \frac{1}{2c^2}(\partial_\tau\boldsymbol{\pi})^2 + i\frac{\lambda}{2}\boldsymbol{\pi}^2\right]\right\} = (\det g)^{(N-1)/2}, \tag{7}$$

where

$$g^{-1}(x,x') = \left[-\nabla^2 - c^{-2}\partial_\tau{}^2 + i\lambda(x)\right]\delta(x - x') \tag{8}$$

is the inverse propagator of the π_i field in the fluctuating λ field. We thus obtain the action

$$S[\sigma,\lambda] = \frac{1}{2}\int dx[(\boldsymbol{\nabla}\sigma)^2 + c^{-2}(\partial_\tau\sigma)^2 + i\lambda\sigma^2] - \frac{3N}{2u_0}\int dx\,(i\lambda - r_0)^2 + \frac{N-1}{2}\mathrm{Tr}\ln g^{-1}. \tag{9}$$

In the limit $N \to \infty$, the action becomes proportional to N (this is easily seen by rescaling the σ field, $\sigma \to \sqrt{N}\sigma$) and the saddle-point approximation becomes exact. For uniform and time-independent fields $\sigma(x) = \sigma$ and $\lambda(x) = \lambda$, the saddle-point action is given by

$$\frac{1}{\beta V}S[\sigma,\lambda] = \frac{i}{2}\lambda\sigma^2 - \frac{3N}{2u_0}(i\lambda - r_0)^2 + \frac{N}{2\beta V}\mathrm{Tr}\ln g^{-1} \tag{10}$$

(we use $N-1 \simeq N$ for large N), with $g^{-1}(q) = \mathbf{q}^2 + \omega_n^2/c^2 + i\lambda$ in Fourier space. $q = (\mathbf{q}, i\omega_n)$, $\omega_n = 2\pi T n$ (n integer) is a bosonic Matsubara frequency, and V denotes the volume of the system. From (10), we deduce the saddle-point equations

$$\sigma m^2 = 0, \quad \sigma^2 = \frac{6N}{u_0}\left(\frac{m^2}{c^2} - r_0\right) - N\int_q g(q), \quad (11)$$

where we use the notation

$$\int_q = \frac{1}{\beta}\sum_{\omega_n}\int_{\mathbf{q}} = \frac{1}{\beta}\sum_{\omega_n}\int \frac{d^2q}{(2\pi)^2} \quad (12)$$

and $m^2 = i\lambda c^2$ ($i\lambda$ is real at the saddle point). These equations show that the component σ of the $\boldsymbol{\varphi}$ field which was singled out plays the role of an order parameter. In the ordered phase, σ is nonzero and $m = 0$. The propagator $g(q) = 1/(\mathbf{q}^2 + \omega_n^2/c^2)$ is gapless, thus identifying the π_i fields as the $N-1$ Goldstone modes associated with the spontaneously broken O(N) symmetry. In the disordered phase, σ vanishes and m determines the gap (or "mass") of the $\boldsymbol{\varphi}$ field as well as the correlation length $\xi = c/m$.

A. Zero temperature

The critical value r_{0c} corresponding to the QCP separating the ordered and disordered phases is obtained by setting $\sigma = m = 0$ in Eqs. (11),

$$r_{0c} = -\frac{u_0}{6}\int_{\mathbf{q}}\int_{\omega}\frac{c^2}{\omega^2 + c^2\mathbf{q}^2} = -\frac{u_0 c\Lambda}{24\pi}, \quad (13)$$

where $\int_\omega = \int_{-\infty}^{\infty}\frac{d\omega}{2\pi}$.

In the disordered phase $r_0 \geqslant r_{0c}$, $\sigma = 0$ and the mass $m_0 = m(T=0)$ is determined by Eqs. (11) and (13),

$$\frac{6}{u_0}\left(\frac{m^2}{c^2} - r_0 + r_{0c}\right) - c^2\int_{\mathbf{q}}\int_{\omega}\left(\frac{1}{\omega^2 + c^2\mathbf{q}^2 + m_0^2} - \frac{1}{\omega^2 + c^2\mathbf{q}^2}\right) = 0, \quad (14)$$

which gives

$$\frac{6m_0^2}{u_0 c^2} + \frac{m_0}{4\pi} = \frac{6}{u_0}(r_0 - r_{0c}). \quad (15)$$

By comparing the two terms on the left-hand side of this equation, we obtain a characteristic momentum scale, the Ginzburg scale $k_G \sim cu_0/24\pi$, which signals the onset of critical fluctuations [26]. In the critical regime, $m_0 \ll ck_G$, we obtain

$$m_0 = \frac{24\pi}{u_0}(r_0 - r_{0c}), \quad (16)$$

which gives $z\nu = 1$, i.e., a correlation-length exponent $\nu = 1$, since the dynamical critical exponent $z = 1$. In the noncritical regime $m_0 \gg ck_G$, $m_0 \sim (r_0 - r_{0c})^{1/2}$ and we recover the classical value $\nu = 1/2$. The anomalous dimension η vanishes to leading order in the large-N limit.

In the ordered phase $r_0 \leqslant r_{0c}$, m_0 vanishes and σ is finite,

$$\sigma^2 = -6N\frac{r_0}{u_0} - N\int_{\mathbf{q}}\int_{\omega}\frac{c^2}{\omega^2 + c^2\mathbf{q}^2} = -\frac{6N}{u_0}(r_0 - r_{0c}). \quad (17)$$

The stiffness is equal to $\rho_s = \sigma^2$ [27].

B. Finite temperatures

At finite temperatures, the system is always disordered ($\sigma = 0$), in agreement with the Mermin-Wagner theorem, and the mass m is obtained from the saddle-point equation

$$\begin{aligned} 0 &= \frac{6}{u_0}\left(\frac{m^2}{c^2} - r_0\right) - \int_q \frac{c^2}{\omega_n^2 + c^2\mathbf{q}^2 + m^2} \\ &= \frac{6}{u_0}\left(\frac{m^2}{c^2} - r_0\right) - \frac{T}{2\pi}\ln\left(\frac{\sinh\frac{c\Lambda}{2T}}{\sinh\frac{m}{2T}}\right) \\ &= \frac{6}{u_0}(r_{0c} - r_0) + \frac{T}{2\pi}\ln\left(2\sinh\frac{m}{2T}\right) + \frac{6m^2}{u_0 c^2}. \end{aligned} \quad (18)$$

In the critical regime the last term can be neglected and we obtain

$$m = 2T\,\mathrm{asinh}\left[\frac{1}{2}\exp\left(\frac{\Delta}{2T}\right)\right], \quad (19)$$

where we have introduced the characteristic energy scale $|\Delta|$ defined by

$$\Delta = \frac{24\pi}{u_0}(r_0 - r_{0c}). \quad (20)$$

Δ corresponds to the $T = 0$ gap m_0 on the disordered side $r_0 > r_{0c}$ of the QCP, and to $-4\pi\rho_s/N$ on the ordered side $r_0 < r_{0c}$ with ρ_s the zero-temperature stiffness (see the discussion in the Introduction). The critical regime is defined by $T, |\Delta| \ll ck_G$.

We can rewrite Eq. (19) as

$$\frac{m}{T} = F_\infty\left(\frac{\Delta}{T}\right), \quad (21)$$

with the universal scaling function

$$F_\infty(x) = 2\,\mathrm{asinh}\left(\tfrac{1}{2}e^{x/2}\right). \quad (22)$$

$F_\infty(x)$ satisfies

$$F_\infty(x) = \begin{cases} e^{x/2} & \text{if } x \to -\infty, \\ 2\,\mathrm{asinh}(1/2) & \text{if } x = 0, \\ x & \text{if } x \to \infty, \end{cases} \quad (23)$$

with $2\,\mathrm{asinh}(1/2) \simeq 0.962\,424$. The three cases in Eq. (23) correspond to the renormalized classical ($m \simeq T e^{-|\Delta|/2T}$), quantum critical [$m \simeq 2\,\mathrm{asinh}(1/2)T$], and quantum disordered ($m \simeq \Delta$) regimes, respectively (see Fig. 1).

C. Pressure

In the large-N limit, the pressure $P = -S[\sigma,\lambda]/\beta V$ is obtained from the saddle-point value of the action,

$$\frac{P}{N} = -\frac{m^2\sigma^2}{2Nc^2} + \frac{3}{2u_0}\left(r_0 - \frac{m^2}{c^2}\right)^2 - \frac{1}{2\beta V}\mathrm{Tr}\ln g^{-1}. \quad (24)$$

Using the results of Appendix A for $\mathrm{Tr}\ln g^{-1}$, in the critical regime we can write the pressure in the scaling form (3) with the universal scaling function

$$\mathcal{F}_\infty(x) = \frac{1}{2\pi}\left[\frac{x^3}{12}\Theta(x) - \frac{x}{4}F_\infty(x)^2 + \frac{1}{6}F_\infty(x)^3 + F_\infty(x)\mathrm{Li}_2(e^{-F_\infty(x)}) + \mathrm{Li}_3(e^{-F_\infty(x)})\right]. \quad (25)$$

$\mathrm{Li}_s(z)$ is a polylogarithm,

$$\mathrm{Li}_s(z) = \sum_{k=1}^{\infty}\frac{z^k}{k^s}, \quad (z\in\mathbb{C},\ |z|<1), \quad (26)$$

and $\Theta(x)$ denotes the step function.

From the definition of $\mathcal{F}_\infty(x)$, we obtain the limiting cases

$$\mathcal{F}_\infty(x) = \begin{cases} \frac{\zeta(3)}{2\pi} & \text{if } x\to-\infty, \\ \frac{2\zeta(3)}{5\pi} & \text{if } x=0, \\ 0 & \text{if } x\to\infty, \end{cases} \quad (27)$$

where $\zeta(z)$ is the Riemann zeta function: $\zeta(3)/2\pi \simeq 0.191\,313$ and $2\zeta(3)/5\pi \simeq 0.153\,051$. To obtain $\lim_{x\to-\infty}\mathcal{F}_\infty(x)$ we use $F_\infty(x)\to e^{x/2}$ for $x\to-\infty$ and $\mathrm{Li}_3(1)=\zeta(3)$. The universal number $\mathcal{F}_\infty(0)$ is obtained noting that $F_\infty(0) = 2\ln\tau$, with $\tau = (1+\sqrt{5})/2 = 2-\tau^{-2}$ the golden mean, and using [28]

$$\mathrm{Li}_2(2-\tau) = \frac{\pi^2}{15} - \frac{1}{4}\ln^2(2-\tau),$$
$$\mathrm{Li}_3(2-\tau) = \frac{4}{5}\zeta(3) + \frac{\pi^2}{15}\ln(2-\tau) - \frac{1}{12}\ln^3(2-\tau). \quad (28)$$

It should be noted that the scaling function $F_\infty(x)$ as well as $\mathcal{F}_\infty(0)$ agree with results obtained from the NLσM in the large-N limit [1,14,28]. This follows from the fact that the linear and nonlinear O(N) models are in the same universality class and therefore exhibit the same critical physics.

III. NPRG APPROACH

The strategy of the NPRG approach is to build a family of theories indexed by a momentum scale k such that fluctuations are smoothly taken into account as k is lowered from the microscopic scale Λ down to 0 [15–17]. This is achieved by adding to the action (1) the infrared regulator

$$\Delta S_k[\boldsymbol{\varphi}] = \frac{1}{2}\sum_{q,i}\varphi_i(-q)R_k(q)\varphi_i(q), \quad (29)$$

so that the partition function

$$Z_k[\mathbf{J}] = \int \mathcal{D}[\boldsymbol{\varphi}]\, e^{-S[\boldsymbol{\varphi}]-\Delta S_k[\boldsymbol{\varphi}]+\int dx\sum_i J_i\varphi_i} \quad (30)$$

becomes k dependent. The k-dependent effective action

$$\Gamma_k[\boldsymbol{\phi}] = -\ln Z_k[\mathbf{J}] + \int dx\sum_i J_i\phi_i - \Delta S_k[\boldsymbol{\phi}] \quad (31)$$

is defined as a modified Legendre transform of $-\ln Z_k[\mathbf{J}]$ which includes the subtraction of $\Delta S_k[\boldsymbol{\phi}]$. Here $\boldsymbol{\phi}(x) = \langle\boldsymbol{\varphi}(x)\rangle$ is the order parameter (in the presence of the external source). The initial condition of the flow is specified by the microscopic scale $k=\Lambda$ where we assume that the fluctuations are completely frozen by the ΔS_k term, so that $\Gamma_\Lambda[\boldsymbol{\phi}] = S[\boldsymbol{\phi}]$. The effective action of the original model (1) is given by $\Gamma_{k=0}$ provided that $R_{k=0}$ vanishes. For a generic value of k, the cutoff function $R_k(q)$ suppresses fluctuations with momentum $|\mathbf{q}|\lesssim k$ or frequency $|\omega_n|\lesssim c_k k$ but leaves unaffected those with $|\mathbf{q}|,|\omega_n|/c_k \gtrsim k$ [here c_k denotes the (renormalized) velocity of the $\boldsymbol{\varphi}$ field]. The variation of the effective action with k is given by Wetterich's equation [29]

$$\partial_t\Gamma_k[\boldsymbol{\phi}] = \tfrac{1}{2}\mathrm{Tr}\left\{\partial_t R_k\left(\Gamma_k^{(2)}[\boldsymbol{\phi}] + R_k\right)^{-1}\right\}, \quad (32)$$

where $t=\ln(k/\Lambda)$. $\Gamma_k^{(2)}[\boldsymbol{\phi}]$ denotes the second-order functional derivative of $\Gamma_k[\boldsymbol{\phi}]$. In Fourier space, the trace involves a sum over momenta and Matsubara frequencies as well as the internal index of the $\boldsymbol{\phi}$ field. We use a regulator function $R_k(q)$ which acts both on momenta and frequencies,

$$R_k(q) = Z_{A,k}\left(\mathbf{q}^2 + \frac{\omega_n^2}{c_k^2}\right) r\left(\frac{\mathbf{q}^2+\omega_n^2/c_k^2}{k^2}\right), \quad (33)$$

where $r(Y) = 1/(e^Y-1)$. The k-dependent constant $Z_{A,k}$ is defined below [Eq. (36)].

When $\boldsymbol{\phi}$ is constant, i.e., uniform and time independent, the effective action coincides with the effective potential,

$$U_k(\rho) = \frac{1}{\beta V}\Gamma_k[\boldsymbol{\phi}]\Big|_{\boldsymbol{\phi}\ \mathrm{const}}. \quad (34)$$

Because of the O(N) symmetry of the effective action Γ_k, the effective potential $U_k(\rho)$ must be a function of the O(N) invariant $\rho = \boldsymbol{\phi}^2/2$. The pressure is then simply defined by

$$P(T) = -U_{k=0}(\rho_0), \quad (35)$$

where $\rho_{0,k}$ denotes the position of the minimum of $U_k(\rho)$ and $\rho_0 = \lim_{k\to0}\rho_{0,k}$.

A. Approximate solution of the flow equation

Because of the regulator term ΔS_k, the vertices $\Gamma^{(n)}_{k,i_1\cdots i_n}(q_1,\cdots,q_n)$ are smooth functions of momenta and frequencies and can be expanded in powers of $\mathbf{q}_i^2/k^2$ and $\omega_{n_i}^2/c_k^2k^2$. Thus if we are interested only in the long-distance (critical) physics, we can use a derivative expansion of the effective action [15,16]. In the following, we consider the ansatz

$$\Gamma_k[\boldsymbol{\phi}] = \int dx\left\{\frac{Z_{A,k}}{2}(\boldsymbol{\nabla}\boldsymbol{\phi})^2 + \frac{V_{A,k}}{2}(\partial_\tau\boldsymbol{\phi})^2 + U_k(\rho)\right\}, \quad (36)$$

which is often referred to as the LPA′. It differs from the local potential approximation (LPA) by the introduction of two field renormalization constants $Z_{A,k}$ and $V_{A,k}$ ($Z_{A,\Lambda}=1$ and $V_{A,\Lambda}=c_0^{-2}$). It is the minimal ansatz beyond the LPA which includes a finite anomalous dimension η at the QCP (see below). Moreover the LPA equation for the potential, and therefore the analog equation in the LPA′, are exact in the large-N limit [30]. To further simplify the analysis, we expand

$U_k(\rho)$ about the position $\rho_{0,k}$ of its minimum,

$$U_k(\rho) = \begin{cases} U_k(\rho_{0,k}) + \frac{\lambda_k}{2}(\rho - \rho_{0,k})^2 & \text{if } \rho_{0,k} > 0, \\ U_k(\rho_{0,k}) + \delta_k \rho + \frac{\lambda_k}{2}\rho^2 & \text{if } \rho_{0,k} = 0. \end{cases} \quad (37)$$

Although the RG equations can also be solved for the full effective potential, the determination of the singular part of the pressure turns out to be extremely difficult in that case [31].

The LPA is known to be very accurate to obtain thermodynamic quantities. It has been used to compute the pressure in the three-dimensional quantum φ^4 theory with Ising symmetry (i.e., $N = 1$) [32,33]. The results compare very well with those of the Blaizot-Méndez-Wschebor approach (BMW)—an elaborated NPRG scheme which preserves the full momentum and frequency dependence of the propagator [34–36]. There are also strong indications that the LPA (or the LPA′) is a good approximation even when it is supplemented by a truncation of the effective potential [Eq. (37)] [37]. As will be shown below, the truncated LPA′ remains accurate—and nearly exact in the renormalized classical regime—in the limit $N \to \infty$ [30,38]. Furthermore, it has also been used to determine the phase diagram of the Bose-Hubbard model in two and three dimensions [8,39,40]: Although a truncation of the effective potential leads to a loss of accuracy, the results remain within 10 percent of the exact ones obtained by quantum Monte Carlo simulation [41,42].

The derivation of the flow equation for $U_k(\rho)$, $Z_{A,k}$, and $V_{A,k}$ is standard [15,16] (the only difference with the classical O(N) model comes from the finite size β in the imaginary-time direction [43,44]). The effective potential satisfies the flow equation

$$\partial_t U_k(\rho) = \frac{1}{2}\int_q \partial_t R_k(q)[G_{k,\mathrm{l}}(q;\rho) + (N-1)G_{k,\mathrm{t}}(q;\rho)], \quad (38)$$

where

$$G_{k,\mathrm{l}}^{-1}(q;\rho) = Z_{A,k}\mathbf{q}^2 + V_{A,k}\omega_n^2 + U_k'(\rho) + 2\rho U_k''(\rho) + R_k(q),$$
$$G_{k,\mathrm{t}}^{-1}(q;\rho) = Z_{A,k}\mathbf{q}^2 + V_{A,k}\omega_n^2 + U_k'(\rho) + R_k(q) \quad (39)$$

determine the longitudinal and transverse parts of the propagator $G_k = (\Gamma_k^{(2)} + R_k)^{-1}$ in a constant field $\boldsymbol{\phi}$,

$$G_{k,ij}(q;\boldsymbol{\phi}) = \frac{\phi_i\phi_j}{2\rho}G_{k,\mathrm{l}}(q;\rho) + \left(\delta_{i,j} - \frac{\phi_i\phi_j}{2\rho}\right)G_{k,\mathrm{t}}(q;\rho). \quad (40)$$

The contribution of $G_{k,\mathrm{t}}$ to $\partial_t U_k$ comes with a factor $N-1$ corresponding to the number of transverse modes. When $\rho_{0,k} > 0$, $U_k'(\rho_{0,k})$ vanishes and these modes become gapless for $R_k(q) \to 0$ (Goldstone modes). The stiffness is given by $\rho_{s,k} = 2Z_{A,k}\rho_{0,k}$ [27]. In the disordered phase, the minimum of $U_k(\rho)$ is located at $\rho_{0,k} = 0$ so that all modes exhibit a gap $m_k = \sqrt{U_k'(0)/V_{A,k}}$ [for $R_k(q) \to 0$] corresponding to a finite correlation length $\xi_k = c_k/m_k$ where $c_k = \sqrt{Z_{A,k}/V_{A,k}}$ ($c_\Lambda = c_0$) is the renormalized velocity (see Sec. III C 1 for a further discussion of the velocity). The actual gap m and correlation length ξ in the disordered phase are obtained for $k = 0$.

The flow equations for $Z_{A,k}$ and $V_{A,k}$ are obtained from the flow equation (32) by noting that

$$Z_{A,k} = \lim_{q\to 0}\frac{\partial}{\partial \mathbf{q}^2}\Gamma_{k,\mathrm{t}}^{(2)}(q;\rho_{0,k}),$$
$$V_{A,k} = \lim_{q\to 0}\frac{\partial}{\partial \omega_n^2}\Gamma_{k,\mathrm{t}}^{(2)}(q;\rho_{0,k}). \quad (41)$$

At the zero-temperature QCP, $Z_{A,k} \sim k^{-\eta}$ and $V_{A,k} \sim k^{-\eta-2(z-1)}$ [45], which allows us to deduce both the anomalous dimension η and the dynamical critical exponent z. The latter is equal to one due to the Lorentz invariance of the action (1) at $T = 0$. The exponent ν can be obtained from the divergence of the correlation length $\xi \sim (r_0 - r_{0c})^{-\nu}$ in the disordered phase as the QCP is approached, or more directly from the escape rate from the fixed point when the system is nearly critical.

The RG equations are given by [46]

$$\begin{aligned} \partial_t \rho_{0,k} &= -\frac{3}{2}I_{k,\mathrm{l}} - \frac{N-1}{2}I_{k,\mathrm{t}} \quad \text{if} \quad \rho_{0,k} > 0, \\ \partial_t \delta_k &= \frac{\lambda_k}{2}(N+2)I_{k,\mathrm{l}} \quad \text{if} \quad \rho_{0,k} = 0, \\ \partial_t \lambda_k &= -\lambda_k^2[9J_{k,\mathrm{ll}}(0) + (N-1)J_{k,\mathrm{tt}}(0)], \\ \partial_t Z_{A,k} &= -2\lambda_k^2\rho_{0,k}\frac{\partial}{\partial \mathbf{p}^2}[J_{k,\mathrm{tl}}(p) + J_{k,\mathrm{lt}}(p)]\Big|_{p=0}, \\ \partial_t V_{A,k} &= -2\lambda_k^2\rho_{0,k}\frac{\partial}{\partial \omega_n^2}[J_{k,\mathrm{tl}}(p) + J_{k,\mathrm{lt}}(p)]\Big|_{p=0}, \end{aligned} \quad (42)$$

while the equation for the thermodynamic potential (per unit volume) $U_k(\rho_{0,k})$ is directly obtained from (38). We have introduced the threshold functions

$$I_{k,\alpha} = \int_q \tilde{\partial}_t G_{k,\alpha}(q;\rho_{0,k}),$$
$$J_{k,\alpha\beta}(p) = \int_q [\tilde{\partial}_t G_{k,\alpha}(q;\rho_{0,k})]G_{k,\beta}(p+q;\rho_{0,k}), \quad (43)$$

with $\alpha,\beta = \mathrm{l},\mathrm{t}$. The operator $\tilde{\partial}_t = (\partial_t R_k)\partial_{R_k}$ acts only on the t dependence of the cutoff function R_k. The propagators $G_{k,\mathrm{l}}(p;\rho_{0,k})$ and $G_{k,\mathrm{t}}(p;\rho_{0,k})$ are given by (39) with $U_k'(\rho_{0,k}) = \delta_k$ and $U_k''(\rho_{0,k}) = \lambda_k$.

The flow equations are solved numerically [47]. Results related to the thermodynamics are discussed in the following section.

B. Universal scaling functions

We first solve the equations at $T = 0$ to determine r_{0c} and obtain the critical exponents ν and η as well as the characteristic energy scale $\Delta \equiv \Delta(r_0)$. For $N = 3$ we find $\nu \simeq 0.699$ and $\eta = 0.0507$, to be compared with the best estimates for the three-dimensional O(3) model obtained from resummed perturbative calculations [48] ($\nu \simeq 0.7060$, $\eta = 0.0333$), Monte Carlo simulations [49] ($\nu \simeq 0.7112$, $\eta = 0.0375$), or the NPRG in the BMW approximation [36] ($\nu \simeq 0.715$, $\eta = 0.040$). For $N = 2$, our results $\nu \simeq 0.613$ and $\eta = 0.0582$ should be compared with the critical exponents of the three-dimensional O(2) model: resummed perturbative calculations [48] ($\nu \simeq 0.6700$, $\eta = 0.0334$), Monte Carlo simulations [50] ($\nu \simeq 0.6717$, $\eta = 0.0381$), NPRG-BMW [36] ($\nu \simeq 0.674$, $\eta = 0.041$). Note that the rather poor estimate

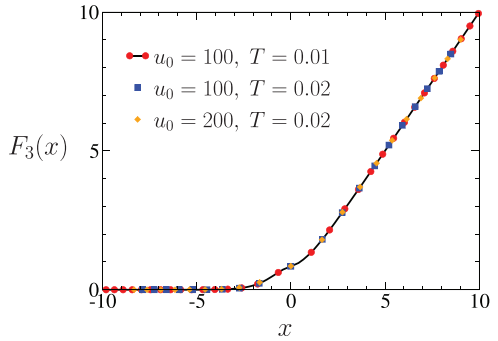

FIG. 2. (Color online) Universal scaling function $F_3(x)$ [Eq. (4)] computed for various values of the microscopic parameters ($\Lambda = 100$ and $c_0 = 1$).

of η is a well-known limitation of the LPA′; a much better result can be obtained by considering the full derivative expansion to order $O(\partial^2)$ [37]. At finite temperatures, the two-dimensional relativistic O(2) model exhibits a BKT phase transition. Although, *stricto sensu*, the NPRG does not capture this transition, most universal properties of the latter are nevertheless correctly reproduced [51,52]. In particular, recent work on the two-dimensional Bose gas has shown that the thermodynamics can be accurately computed using the NPRG [53]. The BKT transition is further discussed in Sec. III E.

Once the QCP is located and the energy scale Δ determined as a function of $r_0 - r_{0c}$, we compute the gap $m(T)$ and the pressure $P(T)$, and deduce the universal scaling functions $F_N(x)$ and $\mathcal{F}_N(x)$ [Eqs. (3) and (4)]. To ensure that we are in the universal (critical) regime, we solve the NPRG equations for various values of the ultraviolet cutoff Λ, interaction strength u_0, or temperature T, and verify that the final results for F_N and $\mathcal{F}_N$ remain unchanged (Figs. 2 and 3). Only at sufficiently low temperatures and close enough to the QCP ($T, |\Delta| \ll ck_G$) do the universal scaling forms (3) and (4) hold.

Figure 4 shows the universal scaling functions F_N and $\mathcal{F}_N$ for various values of N [Table I shows the universal ratio $\rho_s/(N|\Delta|)$]. In the limit $N \to \infty$, the truncated LPA′ slightly differs from the exact result for the excitation gap $m(T)$ but turns out to be extremely accurate for the computation of the pressure $P(T)$ (the LPA′ would be exact without the truncation of $U_k(\rho)$ [38]). For smaller values of N, F_N and $\mathcal{F}_N$ differ significantly from the $N \to \infty$ limit. While the large-N result remains a good approximation in the quantum

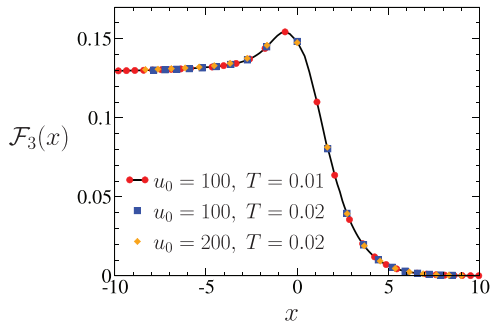

FIG. 3. (Color online) Same as Fig. 2 but for the universal scaling function $\mathcal{F}_3(x)$ [Eq. (3)].

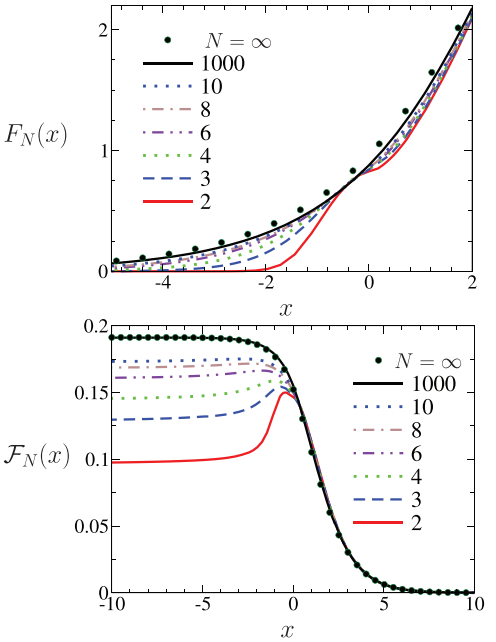

FIG. 4. (Color online) Universal scaling functions F_N and $\mathcal{F}_N$ for various values of N obtained from the NPRG. The black points show the analytic results (22) and (25) in the limit $N \to \infty$.

disordered regime, it becomes inaccurate in the quantum critical and renormalized classical regimes. In particular, it misses the nonmonotonic behavior of $\mathcal{F}_N(x)$ in the quantum critical regime ($|x| \lesssim 1$) for $N \lesssim 10$. The possibility of such a nonmonotonic behavior is discussed in Ref. [54].

In the renormalized classical regime, it is possible to reinterpret the large-N result so that it becomes consistent with the NPRG approach even for small values of N. Since the correlation length ξ is exponentially large, we expect the thermodynamics to be dominated by the $N-1$ modes corresponding to transverse fluctuations to the local order. In the NPRG approach, these modes show up as Goldstone modes as long as $\rho_{0,k} > 0$ (i.e., $k \gtrsim \xi^{-1}$) and dominate the RG flow as in the large-N approach (see the discussion in Sec. III C3 below). Since $N-1$ is identified with N in the large-N approach, the latter overestimates the pressure, and therefore the scaling function $\mathcal{F}_N$, by a factor $N/(N-1)$. In Fig. 5, we show that the large-N result, when rescaled by a factor $(N-1)/N$, is indeed consistent with the NPRG approach. This shows that in the renormalized classical regime

$$P(T) \simeq (N-1)\frac{\zeta(3)}{2\pi}\frac{T^3}{c^2}, \tag{44}$$

which is nothing but the pressure of $N-1$ free bosonic modes with dispersion $\omega = c|\mathbf{q}|$ [55]. The very small excitation gap of the transverse fluctuations ($m \ll T$) does not influence the

TABLE I. Universal ratio $\rho_s/(N|\Delta|)$ in the zero-temperature ordered phase. The exact result in the limit $N \to \infty$ is $1/4\pi \simeq 0.080$.

N	1000	10	8	6	4	3	2
$\rho_s/(N\|\Delta\|)$	0.0838	0.0853	0.0864	0.0891	0.0965	0.1059	0.1321

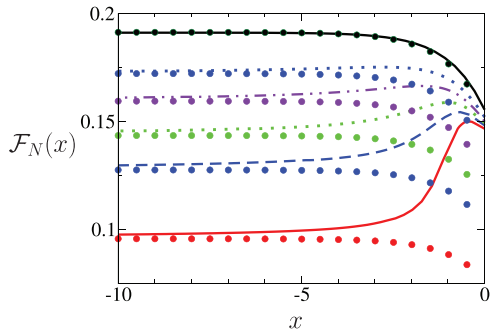

FIG. 5. (Color online) Same as Fig. 4 but for negative values of x only. The dots show the large-N result rescaled by the factor $(N-1)/N$.

thermodynamics. For $N=2$ and $N=3$, Eq. (44) agrees with a RG analysis of the nonlinear sigma model [56,57].

Of particular interest is the temperature variation of the pressure at the QCP ($\Delta=0$). Following Ref. [28], we express the pressure as

$$P(T) = P(0) + \frac{\zeta(3)}{2\pi}\tilde{\mathcal{C}}_N \frac{T^3}{c^2} \tag{45}$$

for $\Delta=0$, where $\tilde{\mathcal{C}}_N = N 2\pi \mathcal{F}_N(0)/\zeta(3)$. In the large-$N$ limit [14],

$$\frac{\tilde{\mathcal{C}}_N}{N} \simeq \frac{4}{5} - \frac{0.3344}{N} + O\left(\frac{1}{N^2}\right) \tag{46}$$

[the leading-order term 4/5 is given by Eq. (27)]. The agreement between the $O(1/N)$ result and the NPRG one rapidly deteriorates for $N \lesssim 10$ (Table II).

The entropy per unit volume is equal to the temperature derivative $\partial P/\partial T$ of the pressure,

$$\frac{S(T)}{V} = N\frac{T^2}{c^2}\left[3\mathcal{F}_N\left(\frac{\Delta}{T}\right) - \frac{\Delta}{T}\mathcal{F}'_N\left(\frac{\Delta}{T}\right)\right]. \tag{47}$$

Up to the factor NT^2/c^2, it is entirely determined by the universal scaling function $3\mathcal{F}_N(x) - x\mathcal{F}'_N(x)$. The latter is nonmonotonic in the quantum critical regime (Fig. 6).

C. RG flows

In this section, we qualitatively discuss the RG flows in the various regimes of the phase diagram in the vicinity of the QCP for $N \geqslant 3$ (Fig. 1). We use the dimensionless variables

$$\begin{aligned} \tilde{\rho}_{0,k} &= k^{1-d}(Z_{A,k}V_{A,k})^{1/2}\rho_{0,k}, \quad \tilde{\delta}_k = (Z_{A,k}k^2)^{-1}\delta_k, \\ \tilde{\lambda}_k &= k^{d-3}Z_{A,k}^{-3/2}V_{A,k}^{-1/2}\lambda_k, \end{aligned} \tag{48}$$

TABLE II. $\tilde{\mathcal{C}}_N/N$ as obtained from the NPRG and the large-N approach [Eq. (46)].

N	1000	10	8	6	4	3	2
$\tilde{\mathcal{C}}_N/N$ to $O(1/N)$	0.800	0.767	0.758	0.744	0.716	0.689	0.633
$\tilde{\mathcal{C}}_N/N$ (NPRG)	0.812	0.796	0.793	0.788	0.781	0.775	0.767

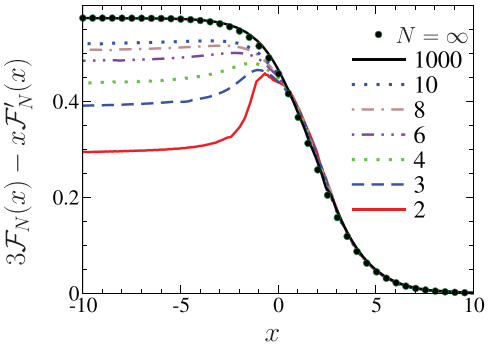

FIG. 6. (Color online) Universal scaling function $3\mathcal{F}_N(x) - x\mathcal{F}'(x)$ for the entropy per unit volume [Eq. (47)].

and the corresponding RG equations

$$\begin{aligned} \partial_t \tilde{\rho}_{0,k} &= (1-d-\eta_k/2-\tilde{\eta}_k/2)\tilde{\rho}_{0,k} \\ &\quad -\frac{3}{2}\tilde{I}_{k,\mathrm{l}} - \frac{N-1}{2}\tilde{I}_{k,\mathrm{t}} \quad \text{if } \tilde{\rho}_{0,k} > 0, \\ \partial_t \tilde{\delta}_k &= (\eta_k - 2)\tilde{\delta}_k + \frac{\tilde{\lambda}_k}{2}(N+2)\tilde{I}_{k,\mathrm{l}} \quad \text{if } \tilde{\rho}_{0,k} = 0, \\ \partial_t \tilde{\lambda}_k &= (d-3+3\eta_k/2+\tilde{\eta}_k/2)\tilde{\lambda}_k \\ &\quad -\tilde{\lambda}_k^2[9\tilde{J}_{k,\mathrm{ll}}(0) + (N-1)\tilde{J}_{k,\mathrm{tt}}(0)], \end{aligned} \tag{49}$$

where

$$\begin{aligned} \eta_k &= 2\tilde{\lambda}_k^2\tilde{\rho}_{0,k}\frac{\partial}{\partial y}[\tilde{J}_{k,\mathrm{ll}}(\tilde{p}) + \tilde{J}_{k,\mathrm{tl}}(\tilde{p})]\Big|_{\tilde{p}=0}, \\ \tilde{\eta}_k &= 2\tilde{\lambda}_k^2\tilde{\rho}_{0,k}\frac{\partial}{\partial \tilde{\omega}_n^2}[\tilde{J}_{k,\mathrm{ll}}(\tilde{p}) + \tilde{J}_{k,\mathrm{tl}}(\tilde{p})]\Big|_{\tilde{p}=0}, \end{aligned} \tag{50}$$

with $\tilde{p} = (\mathbf{p}/k, i\tilde{\omega}_n)$, $y = \mathbf{p}^2/k^2$, $\tilde{\omega}_n = \omega_n/c_k k = 2\pi\tilde{T}_k n$ ($\tilde{T}_k = T/c_k k$). The dimensionless threshold functions $\tilde{I}_{k,\alpha}$ and $\tilde{J}_{k,\alpha\beta}(\tilde{p})$ are defined in Appendix B 1. For the sake of generality, we consider an arbitrary space dimension d.

In the zero-temperature limit, using the results of Appendix B 2 for the threshold functions, we recover the flow equations of the $(d+1)$-dimensional (classical) O(N) model in the LPA′. At the QCP ($r_0 = r_{0c}$), critical fluctuations develop below the Ginzburg momentum scale k_G. In the following, we discuss only the universal part of the flow $k \ll k_G$. Deviations from criticality are characterized by two momentum scales. The first one, $k_\Delta = |\Delta|/c$, is associated to the detuning from the QCP. In the $T=0$ disordered phase, k_Δ^{-1} is nothing but the correlation length. In the $T=0$ ordered phase, $k_\Delta \sim k_J$ is related to the Josephson momentum scale $k_J = \rho_s/c$. The latter separates the critical regime $k_J \ll k \ll k_G$ from the Goldstone regime $k \ll k_J$ dominated by the Goldstone modes. The second characteristic momentum scale is the thermal scale $k_T = 2\pi T/c$ associated to the crossover between the quantum ($k \gg k_T$) and classical ($k \ll k_T$) regimes. The three regimes of the phase diagram (Fig. 1) are defined by $k_T \gg k_\Delta$ (quantum critical), $k_T \ll k_\Delta$ and $r_0 > r_{0c}$ (quantum disordered), $k_T \ll k_\Delta$ and $r_0 < r_{0c}$ (renormalized classical).

1. *Quantum critical regime*

The RG flow in the quantum critical regime is shown in Fig. 7 for $N=3$. The parameters of the microscopic action (1) are chosen such that the initial value Λ of the momentum cutoff

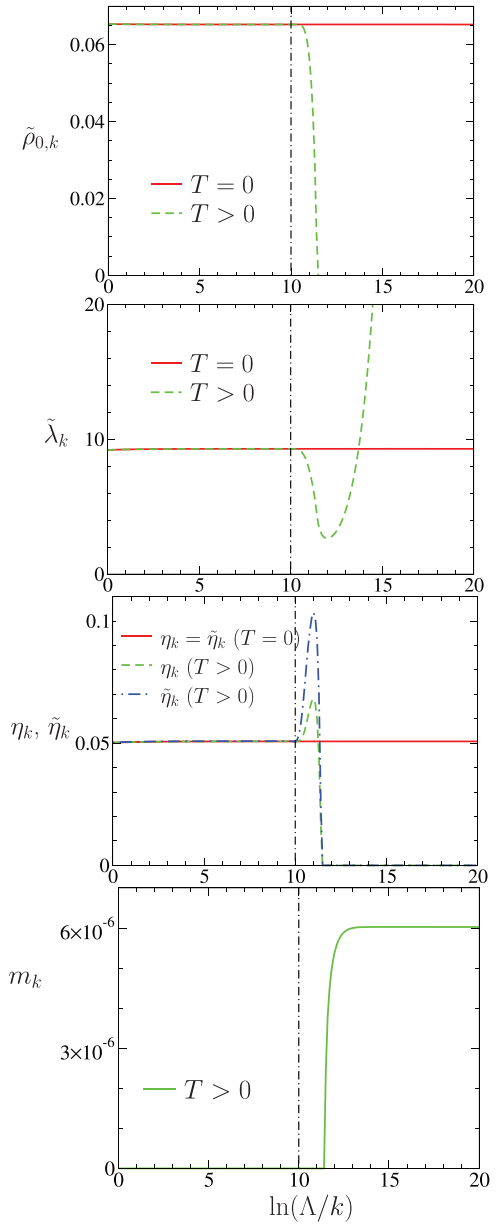

FIG. 7. (Color online) RG flows in the quantum critical regime ($d = 2$ and $N = 3$). The vertical dash-dotted line shows the thermal momentum scale $k_T = \Lambda e^{-10}$. ($\Lambda = c_0 = 1$, $u_0 = 27.6$, $r_{0c} \simeq 0.065\,355$.)

is of the order of the Ginzburg scale k_G. At the QCP ($r_0 = r_{0c}$) and for $T = 0$, we observe plateaus characteristic of critical behavior: $\tilde{\rho}_{0,k} \sim \tilde{\rho}^*_{\rm crit}$, $\tilde{\lambda}_k \sim \tilde{\lambda}^*_{\rm crit}$, and $\eta_k = \tilde{\eta}_k = \eta$ (with η the anomalous dimension at the three-dimensional Wilson-Fisher fixed point). At finite temperatures, the flow is modified when k becomes smaller than the thermal scale k_T: $\tilde{\rho}_{0,k}$ and $\eta_k, \tilde{\eta}_k$ rapidly vanish while $\tilde{\lambda}_k$ diverges; the (dimensionful) order parameter $\rho_{0,k}$ vanishes and $m_k = \sqrt{\delta_k / V_{A,k}}$ takes a finite value (indicating that the system is in a disordered phase). Near k_T, η_k and $\tilde{\eta}_k$ differ, implying a breakdown of Lorentz invariance. It is however difficult to estimate the renormalized value of the velocity. At finite temperature, $V_{A,k}$ gives the coefficient of the ω_n^2 term in the expansion of the vertex $\Gamma^{(2)}_{k,\rm t}(q; \rho_{0,k})$ in powers of ω_n^2. $c_k = \sqrt{Z_{A,k}/V_{A,k}}$ can be identified with the velocity of the (transverse) fluctuations only when $k \gg k_T$. For $k \ll k_T$, the flow is classical (the propagator is dominated by its $\omega_{n=0} = 0$ component) and $V_{A,k}$ does not enter the RG equations anymore. In this regime the actual value $\bar{c}_k$ of the velocity should be obtained from the retarded vertex $\Gamma^{(2)}_{k,\rm t}(\mathbf{q}, \omega; \rho_{0,k}) = U'_k(\rho_{0,k}) + Z_{A,k}(\mathbf{q}^2 - \omega^2/\bar{c}_k^2) + \cdots$ (with ω a real frequency) [58].

2. *Quantum disordered regime*

Figure 8 shows the flow in the quantum disordered regime. At $T = 0$, the critical flow terminates at $k \sim k_\Delta$. For $k \lesssim k_\Delta$, $\tilde{\rho}_{0,k}$ and $\eta_k = \tilde{\eta}_k$ vanish while $\tilde{\lambda}_k$ diverges; the (dimensionful) order parameter $\rho_{0,k}$ vanishes and $m_k = \sqrt{\delta_k / V_{A,k}}$ takes a finite value. As expected, a finite temperature has hardly any

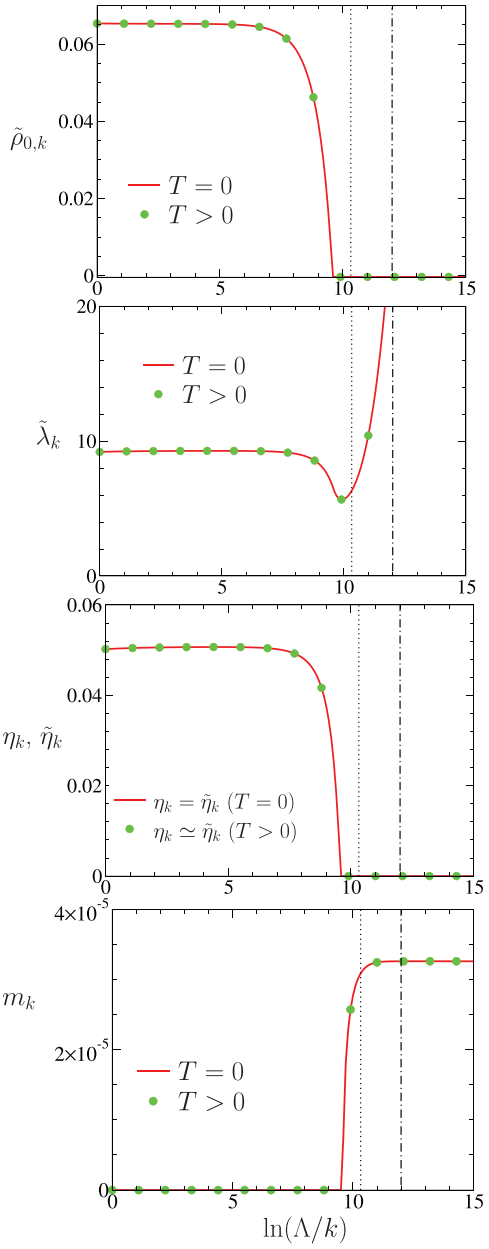

FIG. 8. (Color online) Same as Fig. 7 but in quantum disordered regime [$r_0 = r_{0c}(1 - 10^{-6})$]. The dotted and dash-dotted vertical lines show the momentum scales k_Δ and $k_T = \Lambda e^{-12}$, respectively.

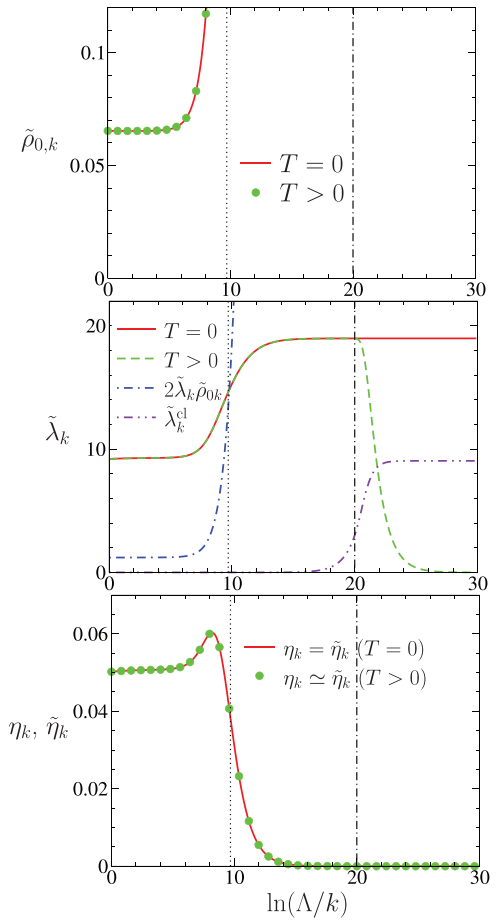

FIG. 9. (Color online) Same as Fig. 7 but in renormalized classical regime [$r_0 = r_{0c}(1 + 10^{-5})$]. The dotted and dash-dotted vertical lines show the momentum scales k_J and $k_T = \Lambda e^{-20}$, respectively.

effect on the flow when $k_T \ll k_\Delta$. Only for $k_T \sim k_\Delta$ (i.e., near the crossover to the quantum critical regime) do we observe a modification of the $T = 0$ flow.

3. *Renormalized classical regime*

The flow in the renormalized classical regime is shown in Fig. 9. The plateaus observed for $k \gg k_J \sim \Lambda e^{-10}$ in $\tilde{\rho}_{0,k}$, $\tilde{\lambda}_k$ and $\eta_k, \tilde{\eta}_k$ show that the behavior of the system at sufficiently high energies (or short distances) is critical. This critical regime terminates at the Josephson scale k_J. For $k \ll k_J$, longitudinal fluctuations are suppressed [the (dimensionless) mass $2\tilde{\lambda}_k\tilde{\rho}_{0,k}$ of the longitudinal mode is much larger than unity] and the flow is dominated by the Goldstone modes. The anomalous dimensions η_k and $\tilde{\eta}_k$ then nearly vanish and the dimensionless interaction $\tilde{\lambda}_k$ exhibits a second plateau whose physical meaning is discussed below. At finite temperatures, this plateau terminates at the thermal scale k_T with $\tilde{\lambda}_k$ vanishing for $k \ll k_T$.

In the Goldstone regime, the flow equations simplify into [59]

$$\begin{aligned} \partial_t \tilde{\rho}_{0,k} &= \left(1 - d - \frac{\eta_k + \tilde{\eta}_k}{2}\right)\tilde{\rho}_{0,k} - \frac{N-1}{2}\tilde{I}_{k,\mathrm{t}}, \\ \partial_t \tilde{\lambda}_k &= (d-3)\tilde{\lambda}_k - \tilde{\lambda}_k^2 (N-1)\tilde{J}_{k,\mathrm{tt}}(0), \end{aligned} \tag{51}$$

where the threshold functions are given in Appendix B 3. $\tilde{\rho}_{0,k}$ becomes very large in the renormalized classical regime. For k smaller than the inverse correlation length ξ^{-1}, $\tilde{\rho}_{0,k}$ will ultimately vanish, but ξ being exponentially large this is not seen in Fig. 9. In Sec. III D we discuss in more detail the behavior of $\tilde{\rho}_{0,k}$ and make the connection with the quantum NLσM.

For $k_T \ll k \ll k_J$ (quantum Goldstone regime), we can take the $T = 0$ limit of the threshold functions (Appendix B 3a). We then find the fixed-point value

$$\tilde{\lambda}^* = \frac{d-3}{(N-1)\tilde{J}_{k,\mathrm{tt}}(0)} = \frac{4\pi^{3/2}}{(N-1)(2-\sqrt{2})}, \tag{52}$$

where the last value is obtained with the exponential cutoff $r(Y) = 1/(e^Y - 1)$ [Eq. (33)] and for $d = 2$. This fixed-point value shows up as a plateau $\tilde{\lambda}_k \simeq \tilde{\lambda}^*$ for $k_T \ll k \ll k_J$, which should not be confused with the plateau $\tilde{\lambda}_k \simeq \tilde{\lambda}^*_{\rm crit}$ corresponding to the critical regime $k_J \ll k \ll k_G$ (Fig. 9). As discussed in detail in Ref. [25], the constant value $\tilde{\lambda}_k \simeq \tilde{\lambda}^*$ and the diverging $\tilde{\rho}_{0,k} \sim k^{1-d}$ (corresponding to a constant value of the order parameter $\rho_{0,k}$) imply a vanishing of the longitudinal propagator in the infrared limit: $G_{\rm l}(p) \sim 1/(\omega_n^2 + c^2\mathbf{p}^2)^{(3-d)/2}$ for $k_T \ll |\mathbf{p}|, |\omega_n|/c \ll k_J$, and $d < 3$ (the vanishing is logarithmic for $d = 3$).

In the classical Goldstone regime $k \ll k_T$, the flow is dominated by classical ($\omega_n = 0$) transverse fluctuations. As a result, the threshold function $\tilde{J}_{k,\mathrm{tt}}$ becomes proportional to $\tilde{T}_k$ (Appendix B 3b) and $\tilde{\lambda}_k$ vanishes linearly with k. Since only the classical component $\boldsymbol{\phi}(\mathbf{r}) \equiv \boldsymbol{\phi}(\mathbf{r}, i\omega_n = 0)$ of the field matters, the effective action (36) becomes

$$\Gamma_k^{\rm cl}[\boldsymbol{\phi}] = \beta \int d^d r \left\{ \frac{Z_{A,k}}{2}(\boldsymbol{\nabla}\boldsymbol{\phi})^2 + \frac{\lambda_k}{2}(\rho - \rho_{0,k})^2 \right\} \tag{53}$$

for $\rho_{0,k} > 0$. Rescaling the field $\boldsymbol{\phi} \to \sqrt{T}\boldsymbol{\phi}$, we obtain the usual form

$$\Gamma_k^{\rm cl}[\boldsymbol{\phi}] = \int d^d r \left\{ \frac{Z_{A,k}}{2}(\boldsymbol{\nabla}\boldsymbol{\phi})^2 + \frac{\lambda_k^{\rm cl}}{2}(\rho - \rho_{0,k})^2 \right\} \tag{54}$$

of the effective action for a classical model in the LPA′, with the coupling constant $\lambda_k^{\rm cl} = T\lambda_k$. The appropriate dimensionless variable

$$\tilde{\lambda}_k^{\rm cl} = \lambda_k^{\rm cl} Z_{A,k}^{-2} k^{d-4} \tag{55}$$

satisfies the RG equation

$$\partial_t \tilde{\lambda}_k^{\rm cl} = (d-4)\tilde{\lambda}_k^{\rm cl} - (N-1)\tilde{J}_{k,\mathrm{tt}}^{\rm cl}(0)\left(\tilde{\lambda}_k^{\rm cl}\right)^2 \tag{56}$$

with the threshold function

$$\tilde{J}_{k,\mathrm{tt}}^{\rm cl} = \tilde{T}_k^{-1}\tilde{J}_{k,\mathrm{tt}}. \tag{57}$$

This equation admits the fixed-point value

$$\tilde{\lambda}^{\rm cl*} = \frac{d-4}{(N-1)\tilde{J}_{k,\mathrm{tt}}^{\rm cl}(0)} = \frac{4\pi}{(N-1)\ln 2}, \tag{58}$$

where the last value is obtained with the exponential cutoff and for $d = 2$.

D. Goldstone regime and NLσM

In the Goldstone regime, the behavior of the system is governed by the Goldstone modes and we expect a description

based on an effective NLσM to be possible. To identify the coupling constant of the effective NLσM [60], we consider the following microscopic action:

$$S[\boldsymbol{\varphi}] = \int_0^\beta d\tau \int d^d r \left\{ \frac{Z_A}{2} (\boldsymbol{\nabla}\boldsymbol{\varphi})^2 + \frac{V_A}{2} (\partial_\tau \boldsymbol{\varphi})^2 + \frac{\lambda}{2} (\rho - \rho_0)^2 \right\} \tag{59}$$

($\rho = \boldsymbol{\varphi}^2/2$), which is analog to the ansatz (36), (37) for the effective action $\Gamma_k[\boldsymbol{\phi}]$. This action can be written in the dimensionless form

$$S[\tilde{\boldsymbol{\varphi}}] = \int_0^{\tilde{\beta}} d\tilde{\tau} \int d^d \tilde{r} \left\{ \frac{1}{2} (\boldsymbol{\nabla}_{\tilde{r}} \tilde{\boldsymbol{\varphi}})^2 + \frac{1}{2} (\partial_{\tilde{\tau}} \tilde{\boldsymbol{\varphi}})^2 + \frac{\tilde{\lambda}}{2} (\tilde{\rho} - \tilde{\rho}_0)^2 \right\}, \tag{60}$$

where $\tilde{\mathbf{r}} = k\mathbf{r}$, $\tilde{\tau} = \sqrt{Z_A/V_A}\, k\tau$, and $\tilde{\boldsymbol{\varphi}}$ is defined in the same way as $\tilde{\boldsymbol{\phi}}$ in Eq. (48). Rescaling the field $\tilde{\boldsymbol{\varphi}} \to \sqrt{2\tilde{\rho}_0}\tilde{\boldsymbol{\varphi}}$, we then obtain

$$S[\tilde{\boldsymbol{\varphi}}] = \tilde{\rho}_0 \int_0^{\tilde{\beta}} d\tilde{\tau} \int d^d \tilde{r} \left\{ (\boldsymbol{\nabla}_{\tilde{r}} \tilde{\boldsymbol{\varphi}})^2 + (\partial_{\tilde{\tau}} \tilde{\boldsymbol{\varphi}})^2 + \frac{\tilde{\lambda}\tilde{\rho}_0}{2} (\tilde{\boldsymbol{\varphi}}^2 - 1)^2 \right\}. \tag{61}$$

In the limit $\tilde{\lambda}\tilde{\rho}_0 \gg 1$, the last term in (61) imposes the constraint $\tilde{\boldsymbol{\varphi}}^2 = 1$, and we obtain a quantum NLσM with dimensionless coupling constant $\tilde{g} = 1/2\tilde{\rho}_0$.

In the NPRG approach, the coupling constant $\tilde{g}_k = 1/2\tilde{\rho}_{0,k}$ satisfies the RG equation

$$\partial_t \tilde{g}_k = -\left(1 - d - \frac{\eta_k + \tilde{\eta}_k}{2}\right) \tilde{g}_k + (N-1) \tilde{I}_{k,\mathrm{t}} \tilde{g}_k^2, \tag{62}$$

which can be deduced from (51). Equation (62) should be considered together with the RG equation of the dimensionless temperature $\tilde{T}_k = T/c_k k$,

$$\partial_t \tilde{T}_k = -\left(1 - \frac{\eta_k - \tilde{\eta}_k}{2}\right) \tilde{T}_k. \tag{63}$$

Following Chakravarty *et al.* [18], we consider the coupling constants $\tilde{g}_k$ and $\tilde{t}_k = \tilde{g}_k \tilde{T}_k$ (rather than $\tilde{g}_k$ and $\tilde{T}_k$), with

$$\partial_t \tilde{t}_k = -(2 - d - \eta_k)\tilde{t}_k + (N-1)\tilde{I}_{k,\mathrm{t}} \tilde{g}_k \tilde{t}_k. \tag{64}$$

In the quantum Goldstone regime $k \gg k_T$, the system is effectively in the zero-temperature limit since $\tilde{T}_k \ll 1$. Let us first consider the theta cutoff function [61]

$$R_k(q) = Z_{A,k} \left(k^2 - \mathbf{q}^2 - \frac{\omega_n^2}{c_k^2}\right) \Theta\left(k^2 - \mathbf{q}^2 - \frac{\omega_n^2}{c_k^2}\right). \tag{65}$$

In that case, one has $2\eta_k \tilde{\rho}_{0,k} = -\tilde{I}_{k,\mathrm{t}}$ (see Appendix B 3c), so that $\tilde{g}_k$ satisfies the flow equation

$$\partial_t \tilde{g}_k = -(1-d)\tilde{g}_k - 2\frac{K_{d+1}}{d+1}(N-2)\tilde{g}_k^2. \tag{66}$$

We have used $\eta_k = \tilde{\eta}_k$ (which holds for $\tilde{T}_k \to 0$) and $\tilde{I}_{k,\mathrm{t}} = -2K_{d+1}/(d+1)$ [with $K_d(2\pi)^d = 4v_d(2\pi)^d$ the surface of the d-dimensional unit sphere]. Equation (66) is nothing but the flow equation of the coupling constant in the $(d+1)$-dimensional classical NLσM [18,62,63]. It agrees with the result of Chakravarty *et al.* to order $\tilde{g}_k^2$ [18]. In particular, we find that the $O(\tilde{g}_k^2)$ term vanishes for the O(2) model ($N = 2$) as expected. Note however that the coefficient of $(N-2)\tilde{g}_k^2$ depends on the RG scheme and may therefore differ from the result of Ref. [18] obtained with a sharp cutoff. For an arbitrary function $R_k(q)$, the equality $2\eta_k\tilde{\rho}_{0,k} = -\tilde{I}_{k,\mathrm{t}}$ is in general violated, which does not allow us to recover the factor $N-2$ in the RG equation $\partial_t \tilde{g}_k$. For example, with the exponential cutoff $r(Y) = 1/(e^Y - 1)$, $-2\eta_k\tilde{\rho}_{0,k}/\tilde{I}_{k,\mathrm{t}} \simeq 1.11$ for $d = 2$. This failure is clearly an artifact of the LPA′. In the regime where Eq. (66) is valid, the $O(\tilde{g}_k^2)$ term is small and the LPA′ remains nevertheless a very good approximation to the flow equation of $\tilde{g}_k$. In one dimension, $\partial_t \tilde{g}_k$ is independent of the choice of the cutoff function R_k to $O(\tilde{g}_k^2)$, in agreement with the fact that the beta function of the classical two-dimensional NLσM is universal (i.e., independent of the RG scheme) to two-loop order [64].

There is a quantum classical crossover when $k \sim k_T$, and for $k \ll k_T$ the system is governed by an effective classical NLσM with coupling constant $\tilde{t}_k$ [18]. With the theta cutoff (65), using $2\eta_k\tilde{\rho}_{0,k} = -\tilde{I}_{k,\mathrm{t}}$ and $\tilde{I}_{k,\mathrm{t}} = -2(K_d/d)\tilde{t}_k/\tilde{g}_k$ (Appendix B 3c), we recover the beta function

$$\partial_t \tilde{t}_k = -(2-d)\tilde{t}_k - 2\frac{K_d}{d}(N-2)\tilde{t}_k^2 \tag{67}$$

of the d-dimensional classical NLσM [18]. As discussed above, for an arbitrary cutoff function $R_k(q)$, the coefficient $N-2$ is not exactly reproduced except for $d = 2$ due to the universality of the beta function $\partial_t \tilde{t}_k$ to two-loop order in that case.

E. O(2) model: BKT transition temperature

In the O(2) model, there is a finite-temperature BKT transition for $r_0 \leqslant r_{0c}$. For the classical O(2) model, the NPRG reproduces most of the universal properties of the BKT transition [51,52]. In particular one finds a value $\tilde{\rho}_0^*$ of the dimensionless order parameter (the spin-wave "stiffness") such that the beta function $\beta(\tilde{\rho}_{0,k}) = \partial_t \tilde{\rho}_{0,k}$ nearly vanishes for $\tilde{\rho}_{0,k} \geqslant \tilde{\rho}_0^*$. This implies the existence of a line of quasifixed points and enables us to identify a low-temperature phase ($T < T_{\mathrm{BKT}}$) where the running of the stiffness $\tilde{\rho}_{0,k}$, after a transient regime, becomes very slow, implying a very large (although not strictly infinite as expected in the low-temperature phase of the BKT transition) correlation length ξ. In this low-temperature phase, the anomalous dimension η_k depends on the (slowly varying) stiffness $\tilde{\rho}_{0,k}$. It takes its largest value $\sim 1/4$ when the RG flow crosses over to the disordered (long-distance) regime (for $\tilde{\rho}_{0,k} \sim \tilde{\rho}_0^*$ and $k \sim \xi^{-1}$), and is then rapidly suppressed as $\tilde{\rho}_{0,k}$ further decreases. On the other hand, the beta function is well approximated by $\beta(\tilde{\rho}_{0,k}) = \mathrm{const} \times (\tilde{\rho}_0^* - \tilde{\rho}_{0,k})^{3/2}$ for $\tilde{\rho}_{0,k} \leqslant \tilde{\rho}_0^*$, and the essential scaling $\xi \sim e^{\mathrm{const}/(T - T_{\mathrm{BKT}})^{1/2}}$ of the correlation length above the BKT transition temperature T_{BKT} is reproduced [52]. Thus, although the NPRG approach does not yield a low-temperature phase with an infinite correlation length, it nevertheless allows us to estimate the BKT transition temperature from the value of $\tilde{\rho}_0^*$. A reasonable estimate of the BKT transition temperature in the two-dimensional XY model has been obtained using the NPRG [65]. The same method has been used to determine T_{BKT} in a two-dimensional Bose gas [53] in very good agreement with Monte Carlo simulations [66,67]. We refer to Ref. [53] for more details

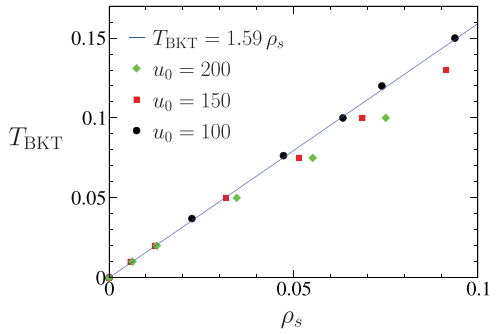

FIG. 10. (Color online) BKT transition temperature $T_{\rm BKT}$ vs the zero-temperature stiffness ρ_s for various values of u_0 ($\Lambda = 100$ and $c_0 = 1$). Sufficiently close to the quantum critical point, the ratio $T_{\rm BKT}/\rho_s \simeq 1.59$ is universal (as shown here by its independence with respect to u_0).

about the determination of the BKT transition temperature in the NPRG approach.

The BKT transition temperature corresponds to an essential singularity in the scaling function $\mathcal{F}_2(x)$. Since $\mathcal{F}_2$ is universal, the ratios $T_{\rm BKT}/|\Delta|$ and $T_{\rm BKT}/\rho_s$ are also universal in the vicinity of the QCP [recall that $\rho_s \equiv \rho_s(T=0)$ is the stiffness in the zero-temperature ordered phase]. The NPRG approach predicts $T_{\rm BKT}/\rho_s \simeq 1.59$ with the exponential cutoff (Fig. 10) and $T_{\rm BKT}/\rho_s \simeq 1.5$ with a theta cutoff $R_k(\mathbf{q}) = Z_{A,k}(k^2 - \mathbf{q}^2)\Theta(k^2 - \mathbf{q}^2)$ acting only on momenta. On the other hand, the ratio $T_{\rm BKT}/\rho_s(T_{\rm BKT}^-) = \pi/2$ is universal anywhere on the transition line, where $\rho_s(T_{\rm BKT}^-)$ denotes the stiffness jump at the transition [68,69]. While our determination of $T_{\rm BKT}$ is not precise enough to yield an accurate estimate of $T_{\rm BKT}/\rho_s$, the latter is close to $\pi/2$, which implies that $\rho_s(T_{\rm BKT}^-)$ is only slightly reduced with respect to the zero-temperature stiffness ρ_s.

More generally, in the low-temperature phase near the QCP we can write the stiffness in the scaling form $\rho_s(T) = \rho_s \mathcal{J}(T/\rho_s)$ with $\mathcal{J}(x)$ a universal scaling function satisfying $\mathcal{J}(0) = 1$. The weak suppression of ρ_s by thermal fluctuations for $T < T_{\rm BKT}$ implies that $\mathcal{J}(x)$ remains close to unity for $x < \pi\rho_s(T_{\rm BKT}^-)/2\rho_s$.

IV. CONCLUSION

Using a NPRG approach, we have obtained the universal function $\mathcal{F}_N$ which determines the scaling form of the pressure near a relativistic QCP with O(N) symmetry [Eq. (3)]. For $N \lesssim 10$, the results are in strong disagreement with the large-N approach both in the renormalized classical and quantum critical regimes. If the large-N approach is properly interpreted, its results in the renormalized classical regime can be reconciled with those of the NPRG approach. It fails however to describe the nonmonotonic behavior of the scaling function $\mathcal{F}_N(x)$ in the quantum critical regime ($|x| \lesssim 1$) as predicted by the NPRG approach. A similar nonmonotonic behavior is observed in the scaling function of the entropy.

We have also shown how the NPRG allows us to obtain a complete picture of the quantum O(N) model in the vicinity of the zero-temperature QCP when $N \geqslant 3$. The characteristic momentum scales k_T and k_Δ, associated with temperature and detuning from the QCP, show up very clearly and yield distinctive RG flows in the quantum critical, quantum disordered, and renormalized classical regimes. In the renormalized classical regime, where the physics is dominated by the $N-1$ Goldstone modes of zero-temperature broken-symmetry phase, the NPRG equations reproduce those of the quantum O(N) NLσM [18].

In the quantum O(2) model, the ratio between the BKT transition temperature $T_{\rm BKT}$ and the zero-temperature stiffness $\rho_s(0)$ is universal near the QCP. The NPRG results show that $T_{\rm BKT}/\rho_s(0)$ is close to the universal ratio $T_{\rm BKT}/\rho_s(T_{\rm BKT}^-) = \pi/2$, implying that the stiffness $\rho_s(T_{\rm BKT}^-)$ at the transition is only slightly reduced with respect to $\rho_s(0)$.

The superfluid–Mott-insulator (at constant density) of a Bose gas in an optical lattice provides us with a well controlled experimental realization of a relativistic QCP with a two-component (complex) field. Recent experiments have shown that it should be possible in the near future to observe quantum criticality associated with this QCP [70]. A measure of the temperature dependence of the pressure in the quantum critical regime would give an experimental estimate of the universal number $\mathcal{F}_2(0)$ and enable a comparison with our theoretical result $\mathcal{F}_2(0) \simeq 0.147$ (i.e., $\tilde{\mathcal{C}}_2/2 \simeq 0.767$). Whether the full scaling function $\mathcal{F}_2(x)$ can be determined in the present experimental conditions requires a detailed study of the relativistic O(2) QCP in the Bose-Hubbard model which will be reported elsewhere.

ACKNOWLEDGMENTS

We would like to thank N. Wschebor and A. Ipp for useful discussions or correspondence.

APPENDIX A: CALCULATION OF Tr ln g^{-1}

In this Appendix, we compute

$$\frac{1}{\beta V}\mathrm{Tr}\ln g^{-1} = \int_q \ln\left(\mathbf{q}^2 + \omega_n^2/c^2 + m^2/c^2\right). \quad \text{(A1)}$$

Since $\mathrm{Tr}\ln g^{-1}$ is divergent, we subtract an infinite constant and consider

$$D(m^2) = \int_q \ln\left(\mathbf{q}^2 + \omega_n^2/c^2 + m^2/c^2\right) - \int_{\mathbf{q}}\int_\omega \ln(\mathbf{q}^2 + \omega^2/c^2). \quad \text{(A2)}$$

It is convenient to write $D(m^2) = D_0(m^2) + D_1(m^2)$, where

$$D_0(m^2) = \int_{\mathbf{q}}\int_\omega [\ln(\mathbf{q}^2 + \omega^2/c^2 + m^2/c^2) - \ln(\mathbf{q}^2 + \omega^2/c^2)], \quad \text{(A3)}$$

and

$$D_1(m^2) = \int_q \ln(\mathbf{q}^2 + \omega_n^2/c^2 + m^2/c^2) - \int_{\mathbf{q}}\int_\omega \ln(\mathbf{q}^2 + \omega^2/c^2 + m^2/c^2). \quad \text{(A4)}$$

Note that $D_1(m^2)$ vanishes at zero temperature.

1. $D_0(m^2)$

Using $D_0(0) = 0$ and

$$D_0'(m^2) = \int_{\mathbf{q}} \int_{\omega} \frac{1}{\omega^2 + c^2\mathbf{q}^2 + m^2} = -\frac{6r_{0c}}{u_0 c^2} - \frac{m}{4\pi c^2}, \tag{A5}$$

we obtain

$$D_0(m^2) = -\frac{6r_{0c}m^2}{u_0 c^2} - \frac{m^3}{6\pi c^2}. \tag{A6}$$

2. $D_1(m^2)$

Given that

$$\frac{1}{\beta}\sum_{\omega_n} \frac{1}{\omega_n^2 + a^2} - \int \frac{d\omega}{2\pi} \frac{1}{\omega^2 + a^2} = \frac{1}{a}\frac{1}{e^{\beta a} - 1} \tag{A7}$$

($a > 0$), we deduce

$$D_1'(m^2) = \int_{\mathbf{q}} \frac{1}{\sqrt{c^2\mathbf{q}^2 + m^2}} \frac{1}{\exp(\beta\sqrt{c^2\mathbf{q}^2 + m^2}) - 1}. \tag{A8}$$

Performing the momentum integral, we then obtain

$$\begin{aligned} D_1'(m^2) &= \frac{1}{2\pi\beta c^2}[-\beta(c\Lambda - m) + \ln(e^{\beta c\Lambda} - 1) \\ &\quad - \ln(e^{\beta m} - 1)] \\ &\simeq \frac{1}{2\pi\beta c^2}[\beta m - \ln(e^{\beta m} - 1)] \end{aligned} \tag{A9}$$

for $T \ll c\Lambda$. From

$$\begin{aligned} D_1'(m^2) &= -\frac{1}{2\pi\beta c^2}\ln(1 - e^{-\beta m}) \\ &= \frac{1}{2\pi\beta c^2}\sum_{k=1}^{\infty} \frac{e^{-k\beta m}}{k}, \end{aligned} \tag{A10}$$

we deduce

$$\begin{aligned} D_1(m^2) &= C - \frac{1}{\pi\beta^3 c^2}\sum_{k=1}^{\infty}\left(\frac{\beta m}{k^2} + \frac{1}{k^3}\right)e^{-k\beta m} \\ &= C - \frac{1}{\pi\beta^3 c^2}[\beta m \mathrm{Li}_2(e^{-\beta m}) + \mathrm{Li}_3(e^{-\beta m})], \end{aligned} \tag{A11}$$

where $\mathrm{Li}_s(z)$ is a polylogarithm [Eq. (26)]. The integration constant C is fixed by requiring $\lim_{m^2\to\infty} D_1(m^2) = 0$. Since $\mathrm{Li}_s(z) \simeq z$ for $|z| \to 0$, this gives $C = 0$.

3. $D(m^2)$

From Eqs. (A6) and (A11), we finally obtain

$$\begin{aligned} D(m^2) &= -\frac{6r_{0c}m^2}{u_0 c^2} - \frac{m^3}{6\pi c^2} \\ &\quad -\frac{1}{\pi\beta^3 c^2}[\beta m \mathrm{Li}_2(e^{-\beta m}) + \mathrm{Li}_3(e^{-\beta m})]. \end{aligned} \tag{A12}$$

Using the same method, we can compute $D(m^2)$ in the fermionic case (which amounts to replacing the bosonic Matsubara frequencies ω_n by fermionic ones). We have verified that we then reproduce the result of Ref. [71] obtained by a different method. The fermionic result differs from the bosonic one only by the sign of the argument of the polylogarithm functions.

APPENDIX B: DIMENSIONLESS THRESHOLD FUNCTIONS

1. Definition

The dimensionless threshold functions [Eq. (50)] are defined by

$$\begin{aligned} \tilde{I}_{k,\alpha} &= 2v_d \int_{\tilde{p}} y^{d/2-1}\big[\eta_k Yr + 2Y^2 r' + (\tilde{\eta}_k - \eta_k)(r + Yr')\tilde{\omega}_n^2\big]\tilde{A}_\alpha^{-2}, \\ \tilde{J}_{k,\alpha\beta}(0) &= 2v_d \int_{\tilde{p}} y^{d/2-1}\big[\eta_k Yr + 2Y^2 r' + (\tilde{\eta}_k - \eta_k)(r + Yr')\tilde{\omega}_n^2\big]\tilde{A}_\alpha^{-2}\tilde{A}_\beta^{-1}, \\ \frac{\partial}{\partial y}\tilde{J}_{k,\alpha\beta}(\tilde{p})\Big|_{\tilde{p}=0} &= -4\frac{v_d}{d}\int_{\tilde{p}} y^{d/2}\big\{2\big[\eta_k Yr + 2Y^2 r' + (\tilde{\eta}_k - \eta_k)(r + Yr')\tilde{\omega}_n^2\big]\tilde{A}'_\alpha\tilde{A}_\alpha^{-3} \\ &\quad - \big[\eta_k r + (\eta_k + 4)Yr' + 2Y^2 r'' + (\tilde{\eta}_k - \eta_k)(2r' + Yr'')\tilde{\omega}_n^2\big]\tilde{A}_\alpha^{-2}\big\}\tilde{A}'_\beta\tilde{A}_\beta^{-2}, \\ \frac{\partial}{\partial\tilde{\omega}_n^2}\tilde{J}_{k,\alpha\beta}(\tilde{p})\Big|_{\tilde{p}=0} &= 2v_d \int_{\tilde{p}} y^{d/2-1}\big[\eta_k Yr + 2Y^2 r' + (\tilde{\eta}_k - \eta_k)(r + Yr')\tilde{\omega}_n^2\big]\big(\tilde{A}_1^2 - \tilde{A}_2\tilde{A}_\beta\big)\tilde{A}_\alpha^{-2}\tilde{A}_\beta^{-3}, \end{aligned} \tag{B1}$$

where

$$\begin{aligned} &\tilde{A}_{\mathrm{t}} = Y(1 + r) + \tilde{\delta}_k, \quad \tilde{A}_1 = \tilde{A}_{\mathrm{t}} + 2\tilde{\lambda}_k\tilde{\rho}_{0,k}, \\ &\tilde{A}'_1 = \tilde{A}'_{\mathrm{t}} = 1 + r + Yr', \end{aligned} \tag{B2}$$

and

$$\begin{aligned} &\tilde{A}_1 = 2\tilde{\omega}_n(1 + r + Yr'), \\ &\tilde{A}_2 = 1 + r + Yr' + 2\tilde{\omega}_n^2(2r' + Yr''). \end{aligned} \tag{B3}$$

We use the notations $v_d^{-1} = 2^{d+1}\pi^{d/2}\Gamma(d/2)$, $Y = y + \tilde{\omega}_n^2$, $r \equiv r(Y)$, $r' \equiv r'(Y)$, $r'' \equiv r''(Y)$, and

$$\int_{\tilde{p}} \equiv \tilde{T}_k \sum_{\tilde{\omega}_n} \int_0^\infty dy. \tag{B4}$$

2. Zero-temperature limit

For $T = 0$, Lorentz invariance implies that $Z_{A,k} = V_{A,k}$ and $\eta_k = \tilde{\eta}_k$. Using

$$\begin{aligned} &v_d \int_0^\infty dy\, y^{d/2-1} \int_{-\infty}^\infty \frac{d\tilde{\omega}}{2\pi} f(Y) \\ &\quad = v_{d+1} \int_0^\infty dY\, Y^{(d+1)/2-1} f(Y) \end{aligned} \tag{B5}$$

for any function $f(Y) = f(y + \tilde{\omega}_n^2)$, we obtain

$$\begin{aligned} \tilde{I}_{k,\alpha} &= 2v_{d+1} \int_0^\infty dY\, Y^{(d+1)/2} (\eta_k r + 2Yr') \tilde{A}_\alpha^{-2}, \\ \tilde{J}_{k,\alpha\beta}(0) &= 2v_{d+1} \int_0^\infty dY\, Y^{(d+1)/2} (\eta_k r + 2Yr') \tilde{A}_\alpha^{-2} \tilde{A}_\beta^{-1}. \end{aligned} \tag{B6}$$

Equation (B5) implies

$$\int_0^\infty dy\, y^{d/2} \int_{-\infty}^\infty \frac{d\tilde{\omega}}{2\pi} f(Y) = \frac{v_{d+3}}{v_{d+2}} \int_0^\infty dY\, Y^{(d+1)/2} f(Y). \tag{B7}$$

Using

$$\frac{v_{d+3}}{v_{d+2}} = \frac{d}{d+1} \frac{v_{d+1}}{v_d}, \tag{B8}$$

we obtain

$$\begin{aligned} &\frac{\partial}{\partial y} [\tilde{J}_{k,\mathrm{lt}}(\tilde{p}) + \tilde{J}_{k,\mathrm{tl}}(\tilde{p})] \Big|_{\tilde{p}=0} \\ &\quad = -8 \frac{v_{d+1}}{d+1} \int_0^\infty dY\, Y^{(d+1)/2} (1 + r + Yr') \tilde{A}_\mathrm{l}^{-2} \tilde{A}_\mathrm{t}^{-2} \\ &\qquad \times \big[Y(\eta_k r + 2Yr')(1 + r + Yr') \big(\tilde{A}_\mathrm{l}^{-1} + \tilde{A}_\mathrm{t}^{-1} \big) \\ &\qquad - \eta_k r - (\eta_k + 4) Yr' - 2Y^2 r'' \big]. \end{aligned} \tag{B9}$$

Equations (B6) and (B9) yield the known RG equations of the $(d+1)$-dimensional (classical) O(N) model in the LPA′.

3. Goldstone regime

In the Goldstone regime $2\tilde{\lambda}_k \tilde{\rho}_{0,k} \gg 1$, longitudinal fluctuations are subleading with respect to the transverse ones. This yields $\tilde{I}_{k,\mathrm{l}} = \tilde{J}_{k,\mathrm{ll}} = 0$,

$$\begin{aligned} \tilde{I}_{k,\mathrm{t}} &= 4v_d \int_{\tilde{p}} y^{d/2-1} Y^2 r' \tilde{A}_\mathrm{t}^{-2}, \\ \tilde{J}_{k,\mathrm{tt}} &= 4v_d \int_{\tilde{p}} y^{d/2-1} Y^2 r' \tilde{A}_\mathrm{t}^{-3}, \end{aligned} \tag{B10}$$

and

$$\begin{aligned} \frac{\partial}{\partial y} \tilde{J}_{k,\mathrm{lt}}(\tilde{p}) \Big|_{\tilde{p}=0} &= \frac{2}{\tilde{\lambda}_k^2 \tilde{\rho}_{0,k}^2} \frac{v_d}{d} \int_{\tilde{p}} y^{d/2} (2r' + Yr'') \frac{1 + r + Yr'}{Y(1+r)^2}, \\ \frac{\partial}{\partial y} \tilde{J}_{k,\mathrm{tl}}(\tilde{p}) \Big|_{\tilde{p}=0} &= -\frac{2}{\tilde{\lambda}_k^2 \tilde{\rho}_{0,k}^2} \frac{v_d}{d} \int_{\tilde{p}} y^{d/2} \frac{1 + r + Yr'}{(1+r)^3} \\ &\quad \times [2r'^2 - (1+r) r''] \end{aligned} \tag{B11}$$

to leading order [we have set $\eta_k = \tilde{\eta}_k = 0$ on the right-hand sides of Eqs. (B10) and (B11)].

a. Quantum Goldstone regime $k_T \ll k$

For $k_T \ll k$ (i.e., $T \ll c_k k$), we can take the zero-temperature limit in (B10) and (B11), which gives

$$\begin{aligned} \tilde{I}_{k,\mathrm{t}} &= 4v_{d+1} \int_0^\infty dY\, Y^{(d-1)/2} \frac{r'}{(1+r)^2}, \\ \tilde{J}_{k,\mathrm{tt}} &= 4v_{d+1} \int_0^\infty dY\, Y^{(d-3)/2} \frac{r'}{(1+r)^3}, \end{aligned} \tag{B12}$$

and

$$\begin{aligned} \frac{\partial}{\partial y} \tilde{J}_{k,\mathrm{lt}}(\tilde{p}) \Big|_{\tilde{p}=0} &= \frac{2}{\tilde{\lambda}_k^2 \tilde{\rho}_{0,k}^2} \frac{v_{d+1}}{d+1} \int_0^\infty dY\, Y^{(d-1)/2} \\ &\quad \times \frac{1 + r + Yr'}{(1+r)^2} (2r' + Yr''), \\ \frac{\partial}{\partial y} \tilde{J}_{k,\mathrm{tl}}(\tilde{p}) \Big|_{\tilde{p}=0} &= -\frac{2}{\tilde{\lambda}_k^2 \tilde{\rho}_{0,k}^2} \frac{v_{d+1}}{d+1} \int_0^\infty dY\, Y^{(d+1)/2} \\ &\quad \times \frac{1 + r + Yr'}{(1+r)^3} [2r'^2 - (1+r) r'']. \end{aligned} \tag{B13}$$

Equations (B12) and (B13) can also be deduced from (B6) and (B9) in the limit $2\tilde{\lambda}_k \tilde{\rho}_{0,k} \gg 1$ and with $\tilde{\delta}_k = 0$.

b. Classical Goldstone regime $k \ll k_T$

For $k \ll k_T$, the Matsubara sums in (B10) and (B11) are dominated by the zero-frequency term $\tilde{\omega}_n = 0$, which gives

$$\begin{aligned} \tilde{I}_{k,\mathrm{t}} &= 4v_d \tilde{T}_k \int_0^\infty dy\, y^{d/2-1} \frac{r'}{(1+r)^2}, \\ \tilde{J}_{k,\mathrm{tt}} &= 4v_d \tilde{T}_k \int_0^\infty dy\, y^{d/2-2} \frac{r'}{(1+r)^3}, \end{aligned} \tag{B14}$$

and

$$\begin{aligned} \frac{\partial}{\partial y} \tilde{J}_{k,\mathrm{lt}}(\tilde{p}) \Big|_{\tilde{p}=0} &= \frac{2}{\tilde{\lambda}_k^2 \tilde{\rho}_{0,k}^2} \frac{v_d}{d} \tilde{T}_k \int_0^\infty dy\, y^{d/2-1} \frac{1 + r + yr'}{(1+r)^2} \\ &\quad \times (2r' + yr''), \\ \frac{\partial}{\partial y} \tilde{J}_{k,\mathrm{tl}}(\tilde{p}) \Big|_{\tilde{p}=0} &= -\frac{2}{\tilde{\lambda}_k^2 \tilde{\rho}_{0,k}^2} \frac{v_d}{d} \tilde{T}_k \int_0^\infty dy\, y^{d/2} \frac{1 + r + yr'}{(1+r)^3} \\ &\quad \times [2r'^2 - (1+r) r'']. \end{aligned} \tag{B15}$$

c. theta cutoff

In this section, we show that with the theta cutoff (65) the relation $2\eta_k \tilde{\rho}_{0,k} = -\tilde{I}_{k,\mathrm{t}}$ is satisfied in the Goldstone regime

(to leading order in $1/\tilde{\lambda}_k\tilde{\rho}_{0,k}$). Equation (65) implies

$$\begin{aligned} r(Y) &= \frac{1-Y}{Y}\Theta(1-Y), \\ r'(Y) &= -\frac{1}{Y^2}\Theta(1-Y) - \frac{1-Y}{Y}\delta(1-Y), \\ r''(Y) &= \frac{2}{Y^3}\Theta(1-Y) + \frac{2}{Y^2}\delta(1-Y) + \frac{1-Y}{Y}\delta'(1-Y). \end{aligned} \tag{B16}$$

At zero temperature, from Eq. (B12) we deduce

$$\tilde{I}_{k,\mathrm{t}} = -8\frac{v_{d+1}}{d+1}. \tag{B17}$$

Since $r(1+r+Yr') = r'(1+r+Yr') = 0$, Eqs. (B13) simplify into

$$\begin{aligned} \frac{\partial}{\partial y}\tilde{J}_{k,\mathrm{lt}}(\tilde{p})\bigg|_{\tilde{p}=0} &= \frac{\partial}{\partial y}\tilde{J}_{k,\mathrm{tl}}(\tilde{p})\bigg|_{\tilde{p}=0} \\ &= \frac{2}{\tilde{\lambda}_k^2\tilde{\rho}_{0,k}^2}\frac{v_{d+1}}{d+1}\int_0^\infty dY\, Y^{(d+1)/2} r''\frac{1+r+Yr'}{(1+r)^2}. \end{aligned} \tag{B18}$$

The product $r''(1+r+Yr')$ is ill defined with the theta cutoff because of the derivative $\delta'(1-Y)$ of the Dirac function in r''. To circumvent this difficulty, we integrate by part,

$$\begin{aligned} \frac{\partial}{\partial y}\tilde{J}_{k,\mathrm{lt}}(\tilde{p})\bigg|_{\tilde{p}=0} &= \frac{\partial}{\partial y}\tilde{J}_{k,\mathrm{tl}}(\tilde{p})\bigg|_{\tilde{p}=0} \\ &= -\frac{2}{\tilde{\lambda}_k^2\tilde{\rho}_{0,k}^2}\frac{v_{d+1}}{d+1}\int_0^1 dY\left\{r'\frac{\partial}{\partial Y}\frac{Y^{(d+1)/2}}{1+r} + \frac{r'^2}{2}\frac{\partial}{\partial Y}\frac{Y^{(d+3)/2}}{(1+r)^2}\right\} = \frac{1}{\tilde{\lambda}_k^2\tilde{\rho}_{0,k}^2}\frac{v_{d+1}}{d+1}, \end{aligned} \tag{B19}$$

where we have used $Y(1+r) = 1$ when $0 \leqslant Y \leqslant 1$. From (B17) and (B19), we deduce $2\eta_k\tilde{\rho}_{0,k} = -\tilde{I}_{k,\mathrm{t}}$.

In the classical Goldstone regime, we retain only the zero-frequency term $\tilde{\omega}_n = 0$ in the Matsubara sums. The calculation of $\tilde{I}_{k,\mathrm{t}}$ and η_k is similar to the $T = 0$ limit with the $(d+1)$-dimensional integrals over Y replaced by d-dimensional integrals over y. Again we find $2\eta_k\tilde{\rho}_{0,k} = -\tilde{I}_{k,\mathrm{t}}$, with

$$\tilde{I}_{k,\mathrm{t}} = 4v_d\tilde{T}_k\int_0^\infty dy\, y^{d/2-1}\frac{r'(y)}{[1+r(y)]^2} = -8\tilde{T}_k\frac{v_d}{d}. \tag{B20}$$

[1] S. Sachdev, *Quantum Phase Transitions*, 2nd ed. (Cambridge University Press, Cambridge, 2011).
[2] D. Podolsky and S. Sachdev, Phys. Rev. B **86**, 054508 (2012).
[3] D. Jaksch, C. Bruder, J. I. Cirac, C. W. Gardiner, and P. Zoller, Phys. Rev. Lett. **81**, 3108 (1998).
[4] M. Greiner, O. Mandel, T. Esslinger, T. W. Hänsch, and I. Bloch, Nature (London) **415**, 39 (2002).
[5] T. Stöferle, H. Moritz, C. Schori, M. Köhl, and T. Esslinger, Phys. Rev. Lett. **92**, 130403 (2004).
[6] I. B. Spielman, W. D. Phillips, and J. V. Porto, Phys. Rev. Lett. **98**, 080404 (2007).
[7] M. P. A. Fisher, P. B. Weichman, G. Grinstein, and D. S. Fisher, Phys. Rev. B **40**, 546 (1989).
[8] A. Rançon and N. Dupuis, Phys. Rev. B **84**, 174513 (2011).
[9] D. Podolsky, A. Auerbach, and D. P. Arovas, Phys. Rev. B **84**, 174522 (2011).
[10] L. Pollet and N. Prokof'ev, Phys. Rev. Lett. **109**, 010401 (2012).
[11] S. Gazit, D. Podolsky, and A. Auerbach, Phys. Rev. Lett. **110**, 140401 (2013).
[12] K. Chen, L. Liu, Y. Deng, L. Pollet, and N. Prokof'ev, Phys. Rev. Lett. **110**, 170403 (2013).
[13] M. Endres, T. Fukuhara, D. Pekker, M. Cheneau, P. Schau, C. Gross, E. Demler, S. Kuhr, and I. Bloch, Nature (London) **487**, 454 (2012).
[14] A. V. Chubukov, S. Sachdev, and J. Ye, Phys. Rev. B **49**, 11919 (1994).
[15] J. Berges, N. Tetradis, and C. Wetterich, Phys. Rep. **363**, 223 (2002).
[16] B. Delamotte, arXiv:cond-mat/0702365.
[17] P. Kopietz, L. Bartosch, and F. Schütz, *Introduction to the Functional Renormalization Group* (Springer, Berlin, 2010).
[18] S. Chakravarty, B. I. Halperin, and D. R. Nelson, Phys. Rev. B **39**, 2344 (1989).
[19] V. L. Berezinskii, Sov. Phys. JETP **32**, 493 (1970); **34**, 610 (1971).
[20] J. M. Kosterlitz and D. J. Thouless, J. of Phys. C **6**, 1181 (1973).
[21] J. M. Kosterlitz and D. J. Thouless, J. Phys. C **7**, 1046 (1974).
[22] Hyperscaling implies that the pressure can be written as $P(T) = P_{\mathrm{reg}} + N(T^3/c^2)\bar{\mathcal{F}}_N(\Delta/T)$ with $\bar{\mathcal{F}}_N$ a universal scaling function. Since the regular part P_{reg} is nearly temperature independent in the critical regime, one obtains Eq. (3) with $\mathcal{F}_N(x) = \bar{\mathcal{F}}_N(x) - x^3\lim_{y\to\infty\times\mathrm{sgn}(x)} y^{-3}\bar{\mathcal{F}}_N(y)$.
[23] If the ultraviolet cutoff respects the Lorentz invariance of the action (1), then the velocity c is equal to the bare velocity c_0.
[24] J. Zinn-Justin, *Phase Transitions and Renormalisation Group* (Oxford University Press, Oxford, 2007).
[25] N. Dupuis, Phys. Rev. E **83**, 031120 (2011).
[26] Note that the Ginzburg momentum scale k_G can be obtained directly from dimensional analysis.
[27] The stiffness ρ_s is defined by the increase $\Delta E = \frac{1}{2}\rho_s\int d^dr(\boldsymbol{\nabla}\mathbf{n})^2$ of the energy when the direction $\mathbf{n}$ of the order parameter slowly varies in space. Equivalently, ρ_s can be defined from the propagator $G_{\mathrm{t}}(\mathbf{q}, i\omega_n = 0) = |\langle\boldsymbol{\varphi}\rangle|^2/\rho_s\mathbf{q}^2$ of the $N-1$ transverse modes [$G_{\mathrm{t}}(q) \equiv g(q)$ in the large-N approach, Eq. (8)].
[28] S. Sachdev, Phys. Lett. B **309**, 285 (1993).
[29] C. Wetterich, Phys. Lett. B **301**, 90 (1993).
[30] M. D'Attanasio and T. R. Morris, Phys. Lett. B **409**, 363 (1997).
[31] The difference between $P(T)$ and $P(0)$ is very small (typically of order $0.1T^3/c^2$). To obtain the pressure at low temperatures, it is therefore necessary to compute $P(T)$ with a very high precision, which is quite difficult numerically when dealing with the full potential.

[32] J.-P. Blaizot, A. Ipp, R. Mndez-Galain, and N. Wschebor, Nucl. Phys. A **784**, 376 (2007).

[33] J.-P. Blaizot, A. Ipp, and N. Wschebor, Nucl. Phys. A **849**, 165 (2011).

[34] J.-P. Blaizot, R. Méndez-Galain, and N. Wschebor, Phys. Lett. B **632**, 571 (2006).

[35] F. Benitez, J. P. Blaizot, H. Chaté, B. Delamotte, R. Méndez-Galain, and N. Wschebor, Phys. Rev. E **80**, 030103(R) (2009).

[36] F. Benitez, J.-P. Blaizot, H. Chaté, B. Delamotte, R. Méndez-Galain, and N. Wschebor, Phys. Rev. E **85**, 026707 (2012).

[37] L. Canet, B. Delamotte, D. Mouhanna, and J. Vidal, Phys. Rev. D **67**, 065004 (2003).

[38] In the $T = 0$ ordered phase, the truncation of the effective potential about $\rho_{0,k}$ gives the exact result for the pressure in the limit $N \to \infty$ [30]. In the renormalized classical regime, where the RG flow remains in the ordered phase down to exponential small values of k, the truncated LPA$'$ is also nearly exact for the computation of the pressure.

[39] A. Rançon and N. Dupuis, Phys. Rev. B **83**, 172501 (2011).

[40] A. Rançon and N. Dupuis, Phys. Rev. A **86**, 043624 (2012).

[41] B. Capogrosso-Sansone, N. V. Prokof'ev, and B. V. Svistunov, Phys. Rev. B **75**, 134302 (2007).

[42] B. Capogrosso-Sansone, S. Giorgini, S. Pilati, L. Pollet, N. Prokof'ev, B. Svistunov, and M. Troyer, New J. Phys. **12**, 043010 (2010).

[43] N. Tetradis and C. Wetterich, Nucl. Phys. B **398**, 659 (1993).

[44] M. Reuter, N. Tetradis, and C. Wetterich, Nucl. Phys. B **401**, 567 (1993).

[45] See Sec. IV A in [8].

[46] Note that $I_{k,\mathrm{t}} = I_{k,\mathrm{l}}$ when $\rho_{0,k} = 0$.

[47] In practice, we use the dimensionless equations introduced in Sec. III C.

[48] A. A. Pogorelov and I. M. Suslov, Sov. Phys. JETP **106**, 1118 (2008).

[49] M. Campostrini, M. Hasenbusch, A. Pelissetto, P. Rossi, and E. Vicari, Phys. Rev. B **65**, 144520 (2002).

[50] M. Campostrini, M. Hasenbusch, A. Pelissetto, and E. Vicari, Phys. Rev. B **74**, 144506 (2006).

[51] M. Gräter and C. Wetterich, Phys. Rev. Lett. **75**, 378 (1995).

[52] G. V. Gersdorff and C. Wetterich, Phys. Rev. B **64**, 054513 (2001).

[53] A. Rançon and N. Dupuis, Phys. Rev. A **85**, 063607 (2012).

[54] A. C. Neto and E. Fradkin, Nucl. Phys. B **400**, 525 (1993).

[55] The argument leading to Eq. (44) assumes that the velocity in the renormalized classical regime is the same as at the QCP (see Sec. III C1).

[56] C. P. Hofmann, arXiv:1306.1944.

[57] C. P. Hofmann, Phys. Rev. B **81**, 014416 (2010).

[58] While a calculation of $\bar{c}_k$ is difficult, as it requires one to analytically continue $\Gamma^{(2)}_{k,\mathrm{t}}(q;\rho_{0,k})$ to real frequencies, we note that $c_k = \sqrt{Z_{A,k}/V_{A,k}}$ varies only weakly when k becomes of the order of k_T (only for $k \ll k_T$ does c_k significantly differ from c_0). If we take $c_{k\sim k_T}$ as an estimate of the renormalized value $\bar{c}_{k=0}$ of the velocity, we conclude that the latter differs only slightly from c_0 in the quantum critical regime. While there is no doubt that $\bar{c}_{k=0} \simeq c_0$ in the quantum disordered regime, the agreement of Eq. (44) with the numerical solution of the flow equations shows that this conclusion also holds in the renormalized classical regime (see also Refs. [56,57]).

[59] Although η_k and $\tilde{\eta}_k$ are very small in the Goldstone regime, the term $(\eta_k + \tilde{\eta}_k)\tilde{\rho}_{0,k}$ is of order 1 and must be kept. It plays a crucial role in the derivation of the quantum NLσM (Sec. III D).

[60] B. Delamotte, D. Mouhanna, and M. Tissier, Phys. Rev. B **69**, 134413 (2004).

[61] At finite temperature, the quantification of the Matsubara frequencies $\omega_n = 2\pi T n$ makes the theta cutoff (65) ill suited, except in the regime $2\pi T > c_k k$ where only classical fluctuations ($\omega_n = 0$) contribute to the flow. Here we use the theta cutoff only for illustrative purpose in the $T = 0$ and $T \gg c_k k$ limits.

[62] D. R. Nelson and R. A. Pelcovits, Phys. Rev. B **16**, 2191 (1977).

[63] A. M. Polyakov, Phys. Lett. B **59**, 79 (1975).

[64] D. H. Friedan, Ann. Phys. (NY) **163**, 318 (1985).

[65] T. Machado and N. Dupuis, Phys. Rev. E **82**, 041128 (2010).

[66] N. Prokof'ev, O. Ruebenacker, and B. Svistunov, Phys. Rev. Lett. **87**, 270402 (2001).

[67] N. Prokof'ev and B. Svistunov, Phys. Rev. A **66**, 043608 (2002).

[68] D. R. Nelson and J. M. Kosterlitz, Phys. Rev. Lett. **39**, 1201 (1977).

[69] The NPRG approach (within the standard approximations used to solve the flow equations) does not allow us to obtain a reliable estimate of $\rho_s(T^-_{\mathrm{BKT}})$ and therefore the ratio $T_{\mathrm{BKT}}/\rho_s(T^-_{\mathrm{BKT}})$.

[70] X. Zhang, C.-L. Hung, S.-K. Tung, and C. Chin, Science **335**, 1070 (2012).

[71] H. Chamati and N. S. Tonchev, Europhys. Lett. **95**, 40005 (2011).